МІНІСТЕРСТВО ОСВІТИ ТА НАУКИ УКРАЇНИ
Національний авіаційний університет
Кафедра конструкції літальних апаратів

ДОПУСТИТИ ДО ЗАХИСТУ
Завідувач кафедри, к.т.н., доцент.
_____Святослав ЮЦКЕВИЧ
«___» _____ 2024 р.

КВАЛІФІКАЦІЙНА РОБОТА
ЗДОБУВАЧА ОСВІТНЬОГО СТУПЕНЯ
«БАКАЛАВР»

Тема: «Рольгангова підлога ближньо-магістрального вантажного літака»

Виконав: _____ **Кирило ЛІМАНЄНКО**

Керівник: д.т.н., професор. _____ **Михайло КАРУСКЕВИЧ**

Нормоконтролер: к.т.н., доц. _____ **Володимир КРАСНОПОЛЬСЬКИЙ**

Київ 2024

MINISTRY OF EDUCATION AND SCIENCE OF UKRAINE
National Aviation University
Department of Aircraft Design

PERMISSION TO DEFEND
Head of the department,
Associate Professor, Phd.
_____ Sviatoslav YUTSKEVYCH
"___" _____ 2024

BACHELOR DEGREE THESIS

Topic: "Roller floor for short range cargo plane"

Fulfilled by: _____ **Kyrylo LIMANIENKO**

Supervisor:
PhD, professor _____ **Mykhailo KARUSKEVYCH**

Standards inspector:
PhD, associate professor _____ **Volodymyr KRASNOPOLSKYI**

Kyiv 2024

НАЦІОНАЛЬНИЙ АВІАЦІЙНИЙ УНІВЕРСИТЕТ

Аерокосмічний факультет
Кафедра конструкції літальних апаратів
Освітній ступінь «Бакалавр»
Спеціальність 134 «Авіаційна та ракетно-космічна техніка»
Освітньо-професійна програма «Обладнання повітряних суден»

ЗАТВЕРДЖУЮ
Завідувач кафедри, к.т.н, доцент.
_____ Святослав ЮЦКЕВИЧ
«___» _____ 2024 р.

ЗАВДАННЯ

на виконання кваліфікаційної роботи здобувача вищої освіти

ЛІМАНЄНКА КИРИЛА ЛЕОНІДОВИЧА

1. Тема роботи: «Рольгангова підлога ближньо-магістрального вантажного літака», затверджена наказом ректора від 15 травня 2024 року № 794/ст.
2. Термін виконання роботи: з 20 травня 2024 р. по 16 червня 2024 р.
3. Вихідні дані до роботи: маса комерційного навантаження 18000 кг, дальність польоту з максимальним комерційним навантаженням 1500 км, крейсерська швидкість польоту 825 км/год, висота польоту 11 км.
4. Зміст пояснювальної записки: вступ, основна частина, що включає аналіз літаків-прототипів і короткий опис проектованого літака, обґрунтування вихідних даних для розрахунку, розрахунок основних льотно-технічних та геометричних параметрів літака, компонування вантажної кабіни, розрахунок центрування літака, спеціальна частина, яка містить розробку рольгангової підлоги ближньо-магістрального вантажного літака.
5. Перелік обов’язкового графічного (ілюстративного) матеріалу: загальний вигляд літака (А1×1), компонувальне креслення фюзеляжу (А1×1), модель і діаграми Ansys.

6. Календарний план-графік:

№	Завдання	Термін виконання	Відмітка про виконання
1	Вибір вихідних даних, аналіз льотно-технічних характеристик літаків-прототипів.	20.05.2024 – 21.05.2024	
2	Вибір та розрахунок параметрів проектованого літака.	22.05.2024 – 23.05.2024	
3	Виконання компонування літака та розрахунок його центрування.	24.05.2024 – 25.05.2024	
4	Розробка креслень по основній частині дипломної роботи.	26.05.2024 – 27.05.2024	
5	Огляд літератури за проблематикою роботи. Аналіз застосування рольгангового обладнання.	28.05.2024 – 29.05.2024	
6	3D моделювання рольгангової секції обладнання вантажної кабіни	30.05.2024 – 31.05.2024	
7	Оформлення пояснювальної записки та графічної частини роботи.	01.06.2024 – 02.06.2024	
8	Подача роботи для перевірки на плагіат.	03.06.2024 – 06.06.2024	
9	Попередній захист кваліфікаційної роботи.	07.06.2024	
10	Виправлення зауважень. Підготовка супровідних документів та презентації доповіді.	08.06.2024 – 10.06.2024	
11	Захист дипломної роботи.	11.06.2024 – 16.06.2024	

7. Дата видачі завдання: 20 травня 2024 року

Керівник кваліфікаційної роботи _____ Михайло КАРУСКЕВИЧ

Завдання прийняв до виконання _____ Кирило ЛІМАНЄНКО

NATIONAL AVIATION UNIVERSITY

Aerospace Faculty
Department of Aircraft Design
Educational Degree "Bachelor"
Specialty 134 "Aviation and Aerospace Technologies"
Educational Professional Program "Aircraft Equipment"

APPROVED BY
Head of Department,
Associate Professor, PhD.
_____ Sviatoslav YUTSKEVYCH
"___" _____ 2024

TASK

for the bachelor degree thesis

KYRYLO LIMANIENKO

1. Topic: "Roller floor for short range cargo plane", approved by the Rector's order № 794/ст from 15 May 2024.
2. Period of work: since 20 May 2024 till 16 June 2024.
3. Initial data: payload 18 tons, flight range with maximum capacity 1500 km, cruise speed 825 km/h, flight altitude 11 km.
4. Content (list of topics to be developed): introduction, main part: analysis of prototypes and brief description of designing aircraft, selection of initial data, wing geometry calculation and aircraft layout, landing gear design, engine selection, center of gravity calculation, special part: design of roller floor for short-range cargo plane.
5. Required material: general view of the airplane (A1×1), layout of the airplane (A1×1), Ansys model and diagrams.

6. Thesis schedule:

№	Task	Time limits	Done
1	Selection of initial data, analysis of flight technical characteristics of prototypes aircrafts.	20.05.2024 – 21.05.2024	
2	Selection and calculation of the aircraft designed parameters.	22.05.2024 – 23.05.2024	
3	Performing of aircraft layout and centering calculation.	24.05.2024 – 25.05.2024	
4	Development of drawings on the thesis main part.	26.05.2024 – 27.05.2024	
5	Cargo cabin equipment application analysis.	28.05.2024 – 29.05.2024	
6	3D modeling of roller equipment section for short-range cargo plane.	30.05.2024 – 31.05.2024	
7	Explanatory note checking, editing, preparation of the diploma work graphic part.	01.06.2024 – 02.06.2024	
8	Submission of the work to plagiarism check.	03.06.2024 – 06.06.2024	
9	Preliminary defense of the thesis.	07.06.2024	
10	Making corrections, preparation of documentation and presentation.	08.06.2024 – 10.06.2024	
11	Defense of the diploma work.	11.06.2024 – 16.06.2024	

7. Date of the task issue: 20 May 2024

Supervisor: _____ Mykhailo KARUSKEVYCH

Student: _____ Kyrylo LIMANIENKO

РЕФЕРАТ

Пояснювальна записка кваліфікаційної роботи бакалавра «Рольгангова підлога ближньо-магістрального вантажного літака»:

65 с., 34 рис., 6 табл., 8 джерел

Дана кваліфікаційна робота присвячена розробці аванпроєкту вантажного літака для ближньомагістральних авіаліній з можливістю транспортування вантажів, що відповідає міжнародним стандартам польотів, нормам безпеки, економічності та надійності, а також розробка рольгангової підлоги ближньо-магістрального вантажного літака.

В роботі було використано методи аналітичного розрахунку, компьютерного проєктування за допомогою CAD/CAM/CAE систем, чисельного моделювання і розрахунку на міцність елементів обладнання.

Практичне значення результату кваліфікаційної роботи полягає в створенні універсальної секції обладнання вантажної кабін, що покращує його експлуатаційні якості.

Матеріали кваліфікаційної роботи можуть бути використані в навчальному процесі та в практичній діяльності конструкторів спеціалізованих проектних установ.

Дипломна робота, аванпроект літака, центрування, рольгангова підлога, розрахунок на міцність, універсальна секція

ABSTRACT

Bachelor degree thesis "Roller floor for short range cargo plane"

65 pages, 34 figures, 6 tables, 8 references

This thesis is dedicated to preliminary design of a cargo plane for short-haul airlines with the possibility of transporting cargo, which meets international flight standards, safety, economy and reliability standards, as well as design of roller floor section for cargo compartment.

The design methodology is based on prototype analysis to select the most advanced technical decisions, engineering calculations to get the technical data of designed aircraft and computer based design using CAD/CAM/CAE systems. In special part the numerical modeling and calculation of the strength is used to estimate stress state of the cargo equipment.

Practical value of the work is to design a universal cargo compartment equipment section, which improves its operational performances.

The materials of the qualification work can be used in the aviation industry and educational process of aviation specialties.

Bachelor thesis, preliminary design, center of gravity calculation, roller floor, strength calculation, universal section

Format	№	Designation	Name	Quantity	Notes
			General documents		
A4	1	NAU 24 04L 00 00 00 05 TW	Task for work	1	
	2	NAU 24 04L 00 00 00 05	Short-range cargo aircraft	2	
A1		Sheet 1	General view	1	
A1		Sheet 2	Fuselage layout	1	
A4	3	NAU 24 04L 00 00 00 05 EN	Short-range cargo aircraft	68	
			Explanatory note		

					NAU 24 04L 00 00 00 05 EN
	Sh.	№ doc.	Sign	Date	

Done by	Limanienko K.L.			Roller floor for short range cargo plane (List of qualification paper)	list	sheet	sheets
Supervisor	Karuskevych M.V.				Q	9	68
St.control.	Krasnopolskyi V.S.						
Head of dep.	Yutskevych S.S.						

404 ASF 134

CONTENT

					NAU 24 04L 00 00 00 05 EN
	Sh.	№ doc.	Sign	Date	
Done by		Limanienko K.L.			Content
Supervisor		Karuskevych M.V.			
St.control.		Krasnopolskyi V.S.			
Head of dep.		Yutskevych S.S.			

list	sheet	sheets
Q	10	68

404 ASF 134

INTRODUCTION

In the modern world of cargo transportation, airplanes have proven themselves to be a reliable and efficient way to transport goods. The cargo aircraft can cover long distances and delivering critical cargo with a certain degree of independence from the geographical factors of the area. And let aviation cargo turnover lose in volume compared to sea and rail transport. The plane is still the fastest method of transportation.

In relation to a cargo aircraft, the key indicators are its flight technical characteristics, namely speed, maximum take-off weight, fuel consumption, geometry of the cargo compartment, as well as the load-bearing capacity of its floor. Various standardized unit load devices have an extensive list of requirements for cargo compartment equipment. To meet these requirements, the elements of the cargo compartment equipment acquire complex structure, which complicates the process of its installation in the cabin and also reduces the reliability of the system, making the potential replacement of its components more labour-intensive.

As a result, the question arises of unifying the equipment of the aircraft cargo cabin, which would, to a certain extent, simplify the installation process and increase the reliability of the system by increasing the degree of interchangeability of its elements, as well as shorten its installation time.

1. PRELIMINARY DESIGN OF SHORT-RANGE AIRCRAFT

1.1. Analysis of prototypes and short description of designed aircraft

When creating a cargo aircraft, it is important to remain in the modern context and analyze global trends in the development of this field of mechanical engineering. Recently, many aircraft manufacturing companies have shown interest in the development and updating of the range of short-haul and medium-haul cargo aircraft. This category of planes is in demand on the market and is an object of interest for both private cargo transportation companies and government agencies of various profiles, from defensive to humanitarian rescue.

The An-178, which is one of the newest transport aircraft produced by the Antonov company, was chosen as the main prototype for creating the aircraft. This aircraft is a response to the changing requirements for short-haul cargo aircraft in modern realities. It is also positioned as an aircraft designed to replace the already outdated An-12. A comparison of the characteristics of this aircraft with world analogues is presented in table 1.1 below.

Table 1.1

Performances of prototypes

Parameter	Kawasaki C-2	Embraer KC-390	An-178
Max payload, kg	36	26	18
Flight range with max paylod	4500	2600	1000
Cruise Altitudes,	11	11	11
Thrust/weight ratio	3.898	3.201	2.834
Number of engines and their type	2 turbofan	2 turbofan	2 turbofan
Take off thrust	275.6	139.26	74.26
Pressure ratio	31.8	36.2	22
Bypass ratio	5.31	4.7	4.95
MTOW	141400	86990	52400

Ending of the table 1.1

1	2	3	4
Landing mass	105000	65400	34400
Empty weight	69000	39400	23820
Fuel fraction	0.254	0.2481	0.3435
Payload fraction	0.2546	0.2988	0.3435
Wing span	44.4	35.05	30.57
Fuselage length	43.9	35.2	32.23
Fuselage diameter	5	4	3.95
Fuselage fineness ratio	8.78	8.8	8.16
Cabin height	4	2.95	2.73

1.2. Brief description of the main parts of the aircraft

1.2.1. Wing

The aircraft has a high-wing configuration. A high-wing design allows the fuselage to be closer to the ground making the cargo loading and unloading operations easier. To improve aerodynamic efficiency and reduce drag, cargo aircraft wings incorporate winglets at the tips. Winglets help enhance fuel efficiency by minimizing vortex formation at the wingtips. Given the cargo-carrying nature of the An-178, the wings are designed with robust structures to withstand the stresses associated with heavy loads. This includes two reinforced wing spars and other structural elements. Aircraft equipped with flaps and slats to enhance lift and control during takeoff and landing. These movable surfaces help optimize the wing's aerodynamic performance in various flight phases. Also wings house fuel tanks to store the aircraft's fuel supply. Smooth fairings and aerodynamic surfaces are incorporated into the wing design to reduce drag and improve overall fuel efficiency. Wing has a supercritical profile optimal for cruise speed of Mach 0.775. And a mean thickness ratio of 0.12.

1.2.2. Fuselage

The aircraft fuselage is built on the principle of semi-monocoque construction. The fuselage structure contains both transverse and longitudinal elements that take on most of the operational loads. The fuselage length is 32.23 meters, and the width is 3.95 meters. There is a cargo ramp at the rear of the fuselage, which simplifies the process of loading luggage into the cabin.

1.2.3. Tail unit

Aircraft features a T-tail arrangement of the empennage meaning that the horizontal stabilizer is located on top of the fin. Such scheme of tail unit is especially useful for aircrafts with high wing configuration due to the risk of conventional tail being susceptible to wake generated by the upper surface of the wing. Introducing the T-tail design solves this problem by lifting the horizontal stabilizer above the zone of risk.

1.2.4. Landing gear

Aircraft features a tricycle landing gear configuration, which includes a single nose semi-articulated landing gear and two main articulated landing gear assemblies in the specially designed fuselage pods. The landing gear is retractable, allowing it to be stowed inside the aircraft during flight. This helps reduce aerodynamic drag, contributing to fuel efficiency. The landing gear incorporates shock absorbers to dampen the impact forces during landing. This feature protects the aircraft structure from excessive stress. The aircraft is equipped with a main landing gear kneeling system intended to simplify loading of the cargo into the aircraft.

1.2.5. Cargo compartment

Cargo compartment of the aircraft is 16.64 (m) long and 2.74 (m) wide. It is able to accommodate various types of cargo including vehicles, paratroopers, unit load devices and cargo pallets. The cargo compartment is spacious enough to fit payload stored inside 96×238.5 inch (2.438×6.058 meters) containers. Also, cargo compartment has 4 equipment mounting tracks located on the floor.

1.2.6. Control system

Aircraft is equipped with a fly-by-wire (FBW) control system, where electronic signals are used to transmit pilot inputs to control surfaces, replacing traditional mechanical linkages. This system enhances flight control precision and allows for advanced automation features. The primary control surfaces include ailerons,

elevators, and rudders. Ailerons control roll (banking left or right), elevators control pitch (nose up or down), and rudders control yaw (side-to-side movement).

1.2.7. Choice and description of power plant

For the designed aircraft two turbofan Д-436Т3 engines will be used. The Д-436 series engines are known for their application in regional jet aircraft, such as the Antonov An-148 and An-158. These turbofan engines are designed to provide a balance of fuel efficiency, reliability, and performance suitable for regional and short-haul flights. They typically feature a two-spool design, advanced materials for improved durability, and modern technologies for enhanced efficiency. Д-436Т3 is a modification of the D-436T1 engine with a take-off thrust of 92185 (N). An increase in the thrust of the engine is ensured by increasing the temperature of the gas in front of the turbine (as in the D-436T2 modification), using a wide-chord low-noise fan (without the support stage) and installing the zero stage of the low-pressure compressor.

Table 1.2

Engine performances

Model	Dry weight	Take-off thrust	Bypass ratio	Pressure ratio	Thrust-specific fuel consumption
Д-436 Т3	1600 kg	92185 N	5	22	10.13 g/kN·s

Conclusions to the analytical part

Based on a comprehensive analysis of selected prototypes, a short-range aircraft with a maximum payload capacity of 18 tons was designed. The An-178 was chosen as the primary prototype for the aircraft developed in this work due to its contemporary design and advanced technological features. The An-178, which had its first flight in May 2015, represents the latest advancements in aviation technology, making it an ideal candidate for serving as a prototype for designed aircraft.

By analyzing and adapting the innovations of the An-178, an aircraft that meets modern standards of efficiency, reliability, and versatility can be developed. This approach ensures that our short-range aircraft not only fulfills its intended operational requirements but also stands out in terms of technological sophistication and market competitiveness.

2. AIRCRAFT MAIN PARTS CALCULATIONS

2.1. Geometry calculations for the main parts of the aircraft

The aircraft configuration is determined by the geometrical properties and arrangement of its components. Aerodynamic layout of the aircraft determines it's aerodynamic and operational characteristics. In order to ensure that aircraft meets all operational, safety requirements, and remains economically efficient. A sufficient portion of attention should be paid to design of aircraft's components. To determine the geometrical properties of designed aircraft it is necessary to analyze the structure of aircraft chosen as prototype.

2.1.1. Wing geometry calculation

Wing area is determined by dividing the aircraft's take-off weight by the maximum load accepted by one square meter of wing area:

$$S_w = \frac{m_0 \cdot g}{P_0} = \frac{64500 \cdot 9.81}{4340} = 117.6\,(\text{m}^2).$$

where m_0 – take-off weight, kg; g – gravity acceleration, m/s^2; P_0 – specific wing load, N/m^2. Relative wing extensions area is 0.01.

Wingspan is a square root of wing area multiplied by wing aspect ratio:

$$l_w = \sqrt{S_w \cdot \lambda_w} = \sqrt{117.6 \cdot 11} = 35.56\,(\text{m}).$$

where λ_w – wing aspect ratio.

Root chord is:

$$b_0 = \frac{2S_w \cdot \eta_w}{(1+\eta_w) \cdot l_w} = \frac{2 \cdot 117.6 \cdot 3.5}{(1+3.5) \cdot 35.56} = 5.03\,(\text{m}).$$

where η_w – wing taper ratio.

Tip chord is:

$$b_t = \frac{b_0}{\eta_w} = \frac{5}{3.5} = 1.44\,(\text{m}).$$

Wing construction and spars position.

The aircraft wing has a two-spar torsion-box structure, which provides an optimal balance between strength and weight. The position of the spars in the wing depends on its current chord. For a wing with two spars, the position of the first will be 20% of the chord from the leading edge. And 60% of the current chord from the leading edge for the second spar.

The spars are shown at the drawing (appendix B).

To determine the mean aerodynamic chord, a geometric method is used (fig. 2.1). The essence of the method is to obtain the position of the average aerodynamic chord at the point of intersection of the rear spar position with the line connecting the length of the root chord laid down from the leading edge of the wingtip with the length of the tip chord laid down from the trailing edge of the root chord.

According to the geometric method for determining the mean aerodynamic chord, its length is 3.56 (m).

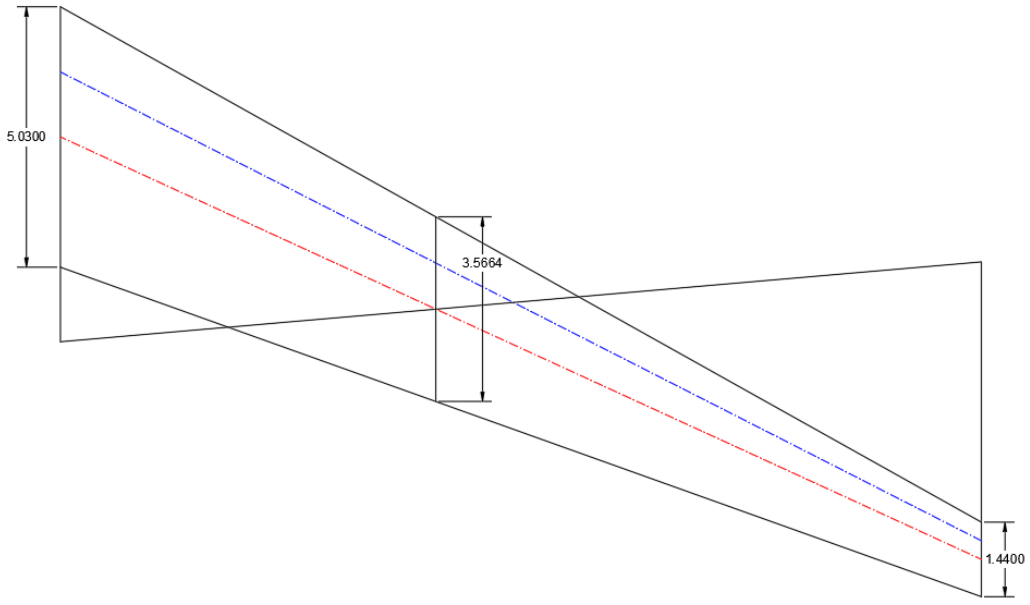

Fig. 2.1. Geometrical method of determination of mean aerodynamic chord.

2.1.2. Fuselage design

The fuselage is specially designed to accommodate the transportation of freight and cargo. The fuselage features a large, unobstructed cargo bay with a reinforced floor to support the weight of various types of cargo. The primary focus of a fuselage is to provide a robust and adaptable space for efficiently transporting a wide range of cargo. Length of the aircraft fuselage:

Forward part of a fuselage requires a streamlined shape for better drag performance. Length of aircraft fuselage forward part is calculated through the following formula:

$$L_{fwd} = FR_{NP} \cdot D_{fus} = 3.95 \cdot 1.75 = 6.9 \text{ (m)}.$$

Tail part of a fuselage is designed for convenient operations with cargo. The main cargo door, located on the fuselage's tail part, is oversized to allow for the easy loading and unloading of large and bulky items. Also, aircraft is equipped with built in cargo ramp. Length of the fuselage tail part:

$$L_{tail} = FR_{TP} \cdot D_{fus} = 3.95 \cdot 3.35 = 13.23 \text{ (m)}.$$

Cargo compartment of the aircraft should be spacious enough to accommodate required payload of 18t. The following dimensions of the cargo compartment were chosen.

Width = 2.76 (m)

Height = 2.74 (m)

Length = 16.64 (m)

2.1.3. Layout and calculation of basic parameters of tail unit

Creating the tail is a very important aspect of developing an aerodynamic layout. The positions of the vertical and horizontal stabilizers determine the directional stability of the aircraft, and to ensure safe maneuvering, the aircraft's centre of gravity must be in front of the aerodynamic centre.

The areas of the horizontal and vertical stabilizer are determined in proportion to the wing area.

Area of vertical tail unit is equal to:

$$S_{HTU} = 0.22 \cdot S_{wing} = 25.3 \ (\text{m}^2).$$

Area of horizontal tail unit is equal to:

$$S_{VTU} = 0.16 \cdot S_{wing} = 18.4 \ (\text{m}^2).$$

Determination of the elevator area and direction:

$$S_{el} = 0.35 \cdot S_{HTU} = 8.855 \ (\text{m}^2).$$

Rudder area:

$$S_{rudder} = 0.25 \cdot S_{HTU} = 3.864 \ (\text{m}^2).$$

Choosing the area of aerodynamic balance.

The area of aerodynamic balance depends on speed of flight. For aircraft with a speed of flight greater than 0.75 Mach the area of aerodynamic balance is found according to proportion:

$$S_{ab\ el} = S_{ab\ \text{rudder}} = 0.19 \cdot S_{control\ \text{surface}}.$$

Elevator balance area is equal:

$$S_{ab\ el} = 0.19 \cdot S_{el} = 1.68 \ (\text{m}^2).$$

Rudder balance area is equal:

$$S_{ab\ \text{rud}} = S_{ab\ el} = 1.68 \ (\text{m}^2).$$

Determination of the tail unit span.

TU span is related to the following dependence:

$$l_{HTU} = 0.32 \cdot l_{wing} = 11.35 \ (\text{m}).$$

The height of the vertical stabilizer is determined depending on the position of the engine. For aircraft whose engine is located at the root of the wing, the height of the vertical stabilizer is in the range of 13%-16% of the wingspan.

$$h_{VTU} = 0.13 \cdot l_{wing} = 4.5 \ (\text{m}).$$

For planes M<1 common tapper ratio of horizontal and vertical tail unit are η_{HTU}=2...3 η_{VTU}=1…1.33

For designed tail unit the following taper ratio values have been chosen; η_{HTU}=3 η_{VTU}=1.25

For transonic planes recommended tail unit aspect ratio is λ_{VTU}=0.8...1.5 Λ_{HTU}=3.5…4.5

Determination of tail unit chords b_{end}, b_{MAC}, b_{root}:

$$b_{tip} = \frac{2 \cdot S_{HTU}}{(\eta_{HTU} + 1) \cdot l_{HTU}} \cdot b_{MAC} = 1.11 \text{ (m)},$$

$$b_{root} = b_{tip} \cdot \eta_{HTU} = 1.11 \cdot 3 = 3.33 \text{ (m)}.$$

For subsonic planes width to chord ratio of the horizontal and vertical tail units is equal to 0.08...0.10. Since the stabilizations fixation is on the fin we need to use upper limit of width to cord ratio, to provide fixation base on the fin. So, width to chord ratio of the horizontal and vertical tail units is equal to C_{TU} = 0.1.

Tail unit sweepback.

Tail unit sweepback is taken in the range 10˚, more than wing sweepback. It is done to provide the control of the airplane in shock stall on the wing. Values of the tail unit sweep are following: Horizontal tail unit 35˚, Vertical tail unit 40˚.

2.1.4. Landing gear design

When designing the landing gear for the aircraft it is necessary to create support that will be stable and reliable for the plane during its taxiing, take-off and landing. The position of landing gear struts not only influences the stability of the aircraft on the ground. But it also influences the load distribution between the nose and main landing gear. The load distribution between nose and main gear depends on it's relative position to the centre of gravity of designed aircraft. Since the aircraft centre of gravity is not determined yet for the designed airplane the main layout of the landing gear is based on prototype.

Main wheel axes offset is:

$$B_m = k_e \cdot b_{MAC} = 0.17 \cdot 3.56 = 0.6\,(\text{m}).$$

where k_e – coefficient of axes offset (k_e = 0.15…0.3); b_{MAC} – mean aerodynamic chord, m.

Aircraft wheel axial offset plays a crucial role in the aircraft stability during taxiing takeoff and landing. A properly designed landing gear offset ensures that aircraft does not tip over when turning on the ground. Also wheel offset influences the ease with which the aircraft's nose lifts off the ground during takeoff, and the control during landing rollout.

Landing gear wheelbase is:

$$B = k_b \cdot L_f = 0.36 \cdot 32.23 = 11.67\,(\text{m}).$$

where k_b – wheelbase calculation coefficient (k_b = 0.3…0.4).

That means that the nose strut holds up to 10% of airplane weight.

Front wheel axial offset is:

$$B_n = B - B_m = 11.67 - 0.6 = 11.07\ (\text{m}).$$

Wheel track is chosen the same as in prototype due to landing gear being attached to the fuselage and being limited to fuselage geometry. $T = 4.35\,(\text{m})$.

The landing gear wheels are chosen based on dimensions and the load experienced during operation, determined by the aircraft's weight. To ensure the proper landing run length the main landing gear is equipped with brakes.

Nose wheel load is:

$$P_{nose} = \frac{9.81 \cdot B_m \cdot k_d \cdot m_0}{B \cdot z} = \frac{9.81 \cdot 0.61 \cdot 1.7 \cdot 64500}{11.67 \cdot 1} = 67944\,(\text{N}).$$

where k_d – dynamics coefficient (k_d = 1.5…2.0); z – number of wheels.

Main wheel load is equal to:

$$P_{main} = \frac{9.81 \cdot (B - B_m) \cdot m_0}{B \cdot n \cdot z} = \frac{9.81 \cdot (11.67 - 11.07) \cdot 64500}{11.67 \cdot 4 \cdot 1} = 148032\,(\text{N}).$$

where n – number of main landing gear struts.

By calculated P_{main} and P_{nose} and the value of $V_{takeoff}$ and $V_{landing,}$ pneumatics is chosen from the catalog, the following correlations should correspond.

$$P^K_{slmain} \geq P_{main}; P^K_{s\ln ose} \geq P_{nose}; V^K_{landing} \geq V_{landing}; V^K_{takeoff} \geq V_{takeoff}$$

Designed aircraft has the following takeoff/landing velocities: $V_{takeoff}$ = 249.42 (km/h), $V_{landing}$ = 233 (km/h). Taking into account loading per each tire the following tires are chosen.

H41×15.0-19 as a main landing gear tire, and 22×8.0-10 as a nose landing gear tires. For ensuring of airplane pass ability, used on the ground runways, pressure in the wheel pneumatics should range in P= (3…5)10^5 (Pa).

Values of tire inflation are 135 (psi) for nose landing gear and 187 (psi) for main landing gear

2.2. Determination of the aircraft center of gravity position

Centering is an important stage in the development of an aircraft, as the position of its center of gravity directly affects its controllability. The position of the center of gravity is influenced not only by the geometry of the aircraft's components but also by the weight and placement of the cargo it carries inside the cabin.

2.2.1. Determination of centering of the equipped wing

The mass of the equipped wing includes the mass of its own structure, encompassing the primary framework and any integral components. This also accounts for the mass of various elements attached to the wing, such as de-icing equipment, navigation lights, and control surfaces. Additionally, the fuel stored within the wing's tanks is a significant contributor to the overall mass. These factors ensure the wing's readiness for operational performance and stability.

The list of the mass objects for the wing is given in the table 2.1. To determine the coordinates of the center of mass for the equipped wing the following formula is used:

$$X'_w = \frac{\sum m'_i \cdot x_i}{\sum m'_i},$$

where X'_w – center of mass for equipped wing, m; m'_i – mass of a unit, kg; x_i – center of mass of the unit, m.

Table 2.1

List of equipped wing masses

#	Object name	Mass		Center of gravity coordinates, m	Moment of mass, kg·m
		Units	Total mass, kg		
1	2	3	4	5	6
1	Wing (structure)	0.15145	9768.525	1.533	14983.06
2	Fuel system	0.0041	264.45	1.569	415.04
3	Flight control system, 30%	0.00198	127.71	2.140	273.32
4	Electrical equipment, 20%	0.00202	130.29	0.356	46.47
5	Anti-icing system, 70%	0.0064	412.8	0.356	147.24
6	Hydraulic system, 30%	0.01239	799.155	2.140	1710.35
7	Power plant	0.0889	5734.05	-3.01	-17259.49
8	Nose landing gear	0.0025	250	3.2	271.711
9	Main landing gear	0.0195	1257.98	14.87	18706.167
10	**Equipped wing without landing gear and fuel**	**0.26724**	**17236.98**	**0.018**	**316.01**
11	Fuel for flight	0.14289	9216.405	1.569	14464.96
12	**Totally equipped wing**	**0.41013**	**26453.4**	**0.558**	**14780.97**

2.2.2. Determination of the centering of the equipped fuselage

Fuselage centering refers to the alignment and positioning of the it's components in relation to its center of gravity and overall aerodynamic design. This involves ensuring that the fuselage is correctly balanced and aligned so that the aircraft maintains optimal performance, stability, and control during all phases of flight. The task of centering is to distribute the masses of structural components of the fuselage. The mass of the equipped fuselage consists of its own framework and equipment, payloads housed within it. In the mass register information about names of the objects and their respective masses and the coordinates of their centers of

gravity. The coordinates system used for this purpose originates at a specific point: the projection of the fuselage nose on the horizontal axis.

To provide a comprehensive overview, table 2.2 lists the various objects that comprise the equipped fuselage. This table serves as a crucial reference, detailing each item's mass and its positional data relative to the established coordinate system. The center of gravity coordinates of the equipped fuselage is determined by formula:

$$X'_f = \frac{\sum m'_i \cdot x_i}{\sum m'_i}.$$

where X'_f – center of mass for equipped fuselage, m; m'_i – mass of a unit, kg; x_i – center of mass of the unit, m.

Table 2.2

List of equipped fuselage masses

#	Object name	Mass		Center of gravity coordinates, m	Moment of mass, kg·m
		Units	Total mass, kg		
1	2	3	4	5	6
1	Fuselage	0.133	8628.81	16.116	139061.9
2	Horizontal tail	0.0175	1130.04	18.2	20566.728
3	Vertical tail	0.02	1290	16.6	21414
4	Nose landing gear	0.0013	84.909	3.2	271.711
5	Main landing gear	0.0195	1257.98	14.87	18706.167
6	Radar	0.0058	374.1	1	374.1
7	Radio equipment	0.0044	283.8	1	283.8
8	Instrument panel	0.0102	657.9	2	1315.8
9	Aero navigation equipment	0.0087	561.15	2	1122.3
10	Flight control system 70%	0.00462	297.99	16.116	4802.406
11	Hydraulic system 30%	0.00531	342.495	22.5624	7727.509
12	electrical equipment 90%	0.01818	1172.61	16.116	18897.78
13	not typical equipment	0.00346	223.17	13.2	2945.84
14	lining and insulation	0.0072	464.4	16.116	7484.27
15	anti ice system, 20%	0.0032	206.4	25.785	5322.14
16	airconditioning system, 40%	0.0064	412.8	16.116	6652.68
17	Furnishing	0.0233	1502.85	3	4508.55
18	Operational items	0.0172	1109.4	13.2	14644.08
19	cargo equipment	0.0007	45.15	16	722.4
20	**equipped fuselage without payload**	**0.31079**	**20045.95**	**13.8**	**276824.2**
21	Payload	0.27908	18000	13.2	237600
22	**TOTAL**	**0.58987**	**38045.95**	**13.52**	**514424.2**

2.2.3. Calculation of center of gravity positioning variants

Estimating the centers of gravity of fuselage and wing, to estimate the centering variants for the aircraft the moment equilibrium equation relatively to the fuselage nose can be made:

$$m_f \cdot X'_f + m_w(X_{MAC} + X'_w) = m_0(X_{MAC} + C).$$

where m_0 – aircraft take-off mass, kg; m_f – mass of equipped fuselage, kg; m_w – mass of equipped wing, kg; C – distance from MAC leading edge to the center of gravity.

Now it is possible to find the wing mean aerodynamic chord leading edge position relative to fuselage nose, This is done using the formula:

$$X_{MAC} = \frac{m_f \cdot X'_f + m_w \cdot X'_w - m_0 \cdot C \cdot b_{MAC}}{m_0 - m_w},$$

$$X_{MAC} = \frac{38046 \cdot 13.52 + 26453 \cdot 0.558 - 64500 \cdot 1.07}{64500 - 26453.4} = 12.1\,(\text{m}).$$

The list of mass objects for center of gravity variants calculation is given in table 2.3 and center of gravity calculation variants are given in table 2.4.

Table 2.3

Calculation of center of gravity position variants

#	Object name	Mass, kg	Center of gravity coordinates, m	Moment of mass, kg·m
1	2	3	4	5
1	Equipped wing without landing gear and fuel	17237	12.113	208801.7
2	Nose landing gear (extended)	84.909	3.2	271.71
3	Main landing gear (extended)	1257.980	14.87	18706.16
4	Fuel reserve	2223.057	13.664	30377.49
5	Fuel for flight	6944.07	13.664	94888.91
6	Equipped fuselage (without payload)	20046	13.809	276824.18
7	Payload	18000	13.2	237600
8	Nose landing gear (retrected)	84.909	2.8	237.747
9	Main landing gear (retrected)	1257.98	14.87	18706.167

Table 2.4

Aircraft's center of gravity position variants

#	Variant of loading	Mass, kg	Moment of mass, kg·m	Center of gravity coordinates, m	Centering, %
1	2	3	4	5	6
1	Take-off mass (landing gear extended)	65792.95	867470.24	13.184	30.54
2	Take-off mass (landing gear retracted)	65792.95	867436.28	13.184	30.53
3	Landing variant (landing gear extended)	58848.9	772581.33	13.128	28.95
4	Transportation variant (without payload)	47792.9	629836.28	13.178	30.36
5	Parking variant (without fuel and payload)	40848.8	534981.33	13.096	28.07

Conclusions to the project part

In this part, the centering of the designed aircraft was performed, also geometrical parameters of main airplane components were calculated. To ensure the aircraft meets all operational requirements. During calculation various operational factors such as the aircraft's intended purpose, the maximum weight of cargo, the expected flight speed and altitude, as well as the conditions for landing and take-off were considered. As a result, all obtained values meat to the requirements for short-range cargo aircraft.

Furthermore, the centering of the designed plane was evaluated. The most forward position of the center of gravity of the fully equipped aircraft is calculated to be 28.07% of the mean aerodynamic chord during flight. Conversely, the most aft position of the aircraft's center of gravity is determined to be 30.54% of the mean aerodynamic chord. These values establish a range within which the aircraft is properly balanced and centered, ensuring optimal stability and performance throughout its operation.

3. ROLLER FLOR FOR SHORT RANGE CARGO PLANE

3.1. Introduction

The process of loading baggage into an aircraft is quite complex and involves several stages. In the case of transporting mobile cargo such as vehicles, they can drive into the cargo compartment using the cargo ramp. However, not all types of cargo can be loaded into the cabin this way. Transporting and loading typical standardized aviation packaging units requires specific equipment adaptations to ensure proper loading. Usually, aviation packaging units and typical cargo are prepared for air transport in advance. After preparation, they are delivered to the aircraft using specialized transport vehicles. The process of loading baggage into the cabin itself does not always allow the use of a cargo ramp. Among other constraints affecting the loading process, attention must also be given to the strength of the container or pallet used for transporting the cargo. These transport means are typically made from thin layers of 7075-T6 aluminum alloy, not exceeding 4.8 mm in thickness. While this structure helps reduce the weight of the container, it significantly limits the use of the aircraft ramp. At certain stages of aircraft loading, the container or pallet needs to transfer from the ramp surface to the floor surface, which the thin-walled structure of the bottom cannot withstand, bending under its own weight. To bypass this limitation, special loading equipment like K-loaders has been developed, allowing the cargo to be lifted to align vertically with the floor level, thus eliminating the process of tipping the container through the root part of the ramp. Such loading equipment is especially necessary for cargo aircraft models converted from passenger ones. Originally designed for passenger transportation, these models have a sufficiently large clearance between the fuselage and the floor level, making such equipment a mandatory tool. Additionally, converted aircraft have a floor level higher than the midsection of the fuselage, necessitating the inclusion of built-

in ramps in K-loaders to close the gap formed between the cargo compartment floor and the surface of the K-loader. For cargo aircraft equipped with a ramp for loading standardized baggage, it is enough to lower the ramp to a level where its surface is parallel to the floor, thereby eliminating the process of tipping the cargo through the root part of the ramp.

Subsequently, the cargo is moved within the cabin along the roller floor and secured at the designated point of the cargo compartment. This is achieved by using cables, as well as bar locks and end locks.

3.2. Universal roller floor section design in the CAM environment "Ansys"

The basis for the created roller floor equipment was taken from a real prototype of equipment intended for transporting pallets 88×108 inches (2.235×2.743 meters), 96×125 inches (2.438×3.175 meters), as well as UAK-10 containers and ISO containers placed on pallets 96×238.5 inches (2.438×6.058 meters). This equipment includes 7 roller sections, 6 sections of locking beams, 3 roller sections for installation on a ramp, as well as a transfer roller designed for installation on a ramp.

The task of the equipment being created will be to facilitate the loading of containers and pallets into the cabin, as well as to hold and secure them during the flight.

When creating a universal roller floor section, the main geometric parameters were selected in such a way that when transporting an 88×108 inches container, exactly 8 universal sections were needed to hold and secure it. When transporting larger containers, a special module of two additional rollers is used, which is attached to the end of the structure opposite to the end lock.

Roller

The roller is mounted on bearings, installed on a bolt that serves as its axle for rotation. The roller is designed to reduce the amount of effort required to move cargo through the cabin by converting sliding friction into rolling friction. For the created

roller floor section, a hollow metal roller with a diameter of 42 millimeters and a width of 64 millimeters is used. The roller 3D model can be seen on figure 3.2.

Fig. 3.2. Roller 3D model.

Roller Bolt

The 9 centimeters long bolt serves as the axle for the roller it withstands bending loads exerted by the cargo. This component is made of structural steel grade 30ХГСА. The diameter of the bolt is 8 mm, and at the points where it is installed in the roller section profile, the use of a bushing is required. After assembling of the roller, the assembly is fixed with a nut. The bolt 3D model can be seen on figure 3.3.

Fig. 3.3. Roller bolt 3D model.

Bushing

The bushing is made of steel grade 12Х18Н10Т-Б. This component serves as a connecting link between the profile of the roller section and the bolt. The bushing

absorbs part of the loads acting on the bolt. The outer diameter of the bushing is 10 (mm), the inner diameter is 8 (mm), and the length of the bushing is 6 (mm). The bushing 3D model can be seen on figure 3.4.

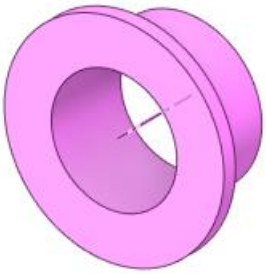

Fig. 3.4. Bushing 3D model.

End lock

This element is located at the end of the roller section. It is made of structural steel 30ХГСА and is necessary for securing the load on the roller section. The end lock absorbs longitudinal loads acting on the cargo during maneuvers and during landing. This element fixes the bottom of the container by the edge in the vertical direction. The height of the end lock must be selected in such a way that the minimum vertical distance between the fixing surface and the extreme height of the roller is 32 (mm), which will ensure reliable grip of the load by the edge of the bottom. Also, when choosing the geometric parameters of the end lock, it is necessary to take into account the bending moment acting on the lock, the value of which increases in proportion to its height. For the created roller section, this element is movable to be able to fold it inside the profile of the roller section in order to prevent it from interfering with the loading of the container during the stages of passing over it. To do this, this lock is mounted on an axis that allows it to rotate. In the folded position, the lock assumes a horizontal position inside the profile of the roller section. The rotational movement around the axis is carried out exclusively in the direction opposite to the nearest roller in order to prevent the lock from being blocked by the bottom of the pallet. To fix the lock in a vertical position, a special fixator is provided that limits its movement when the lock is extended. The end lock 3D model can be seen on figure 3.5. and figure 3.6.

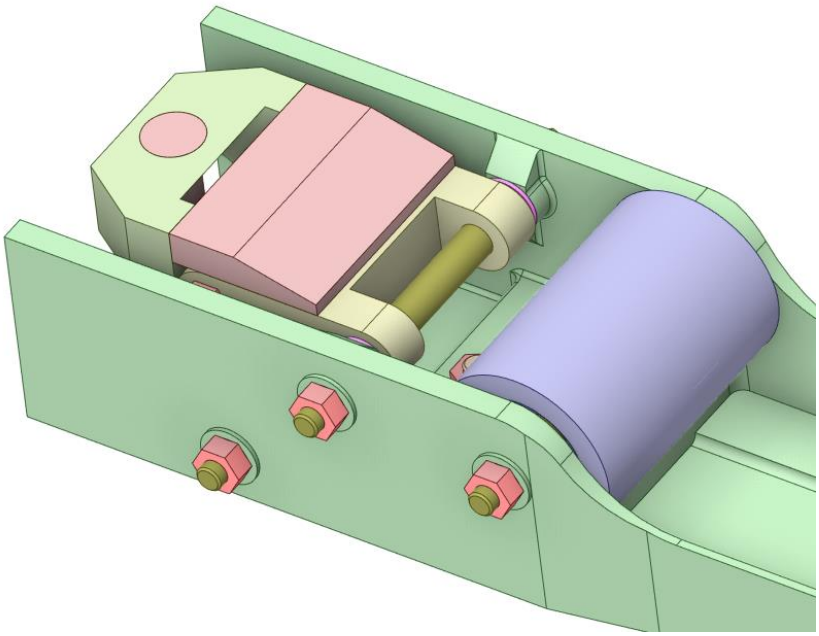

Fig. 3.5. Lowered End Lock 3D model.

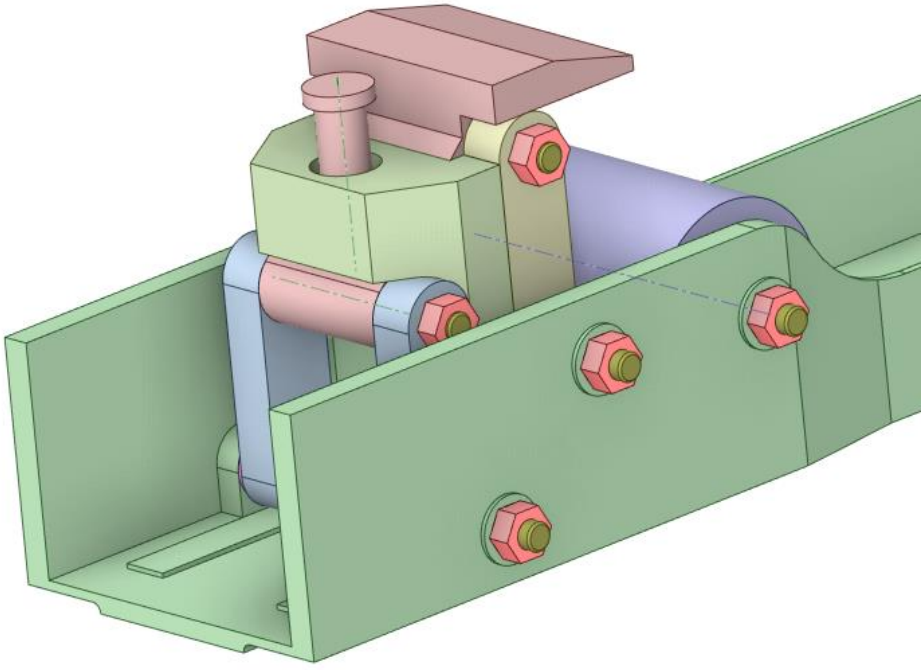

Fig. 3.6. Extended End Lock 3D model.

Vertical fixator

The vertical fixator is made of structural steel 30ХГСА-Б. This element is designed to fix the roller section in the vertical direction by attaching it to the chair rail. The unit is designed to absorb vertical loads arising from the end lock; therefore, these elements are located as close to each other as possible. This element has a hexagonal shape to prevent rotation of the element to maintain its orientation parallel to the roller section. The assembly is inserted into a specially designated hole in the roller section at the bottom of the roller section and secured with a threaded nut at the top of the assembly. The vertical fixator 3D model can be seen on figure 3.7.

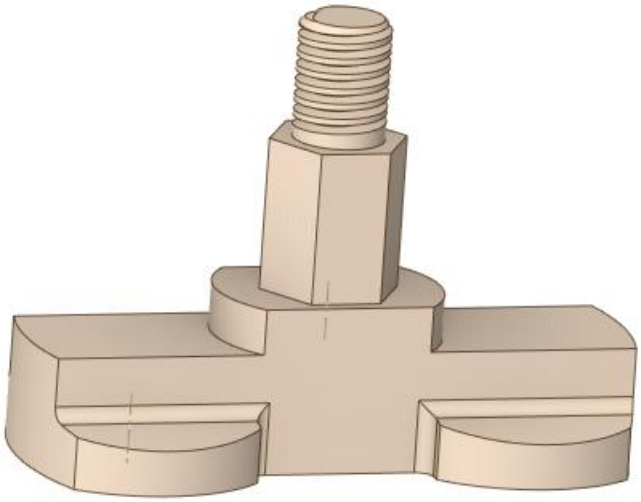

Fig. 3.7. Vertical fixator 3D model.

Three-plug node

This element is made of structural steel 30ХГСА. Its task is to fix the roller section in the longitudinal direction. The fixation is carried out geometrically due to the identical geometry of the plugs and the teeth of the chair rail. Inside the assembly there is an element similar to a vertical fixator, mounted on a spring-loaded axis. Its task is to press the three-plug assembly to the chair rail to avoid its disconnection. The three plug node 3D model can be seen on figure 3.8.

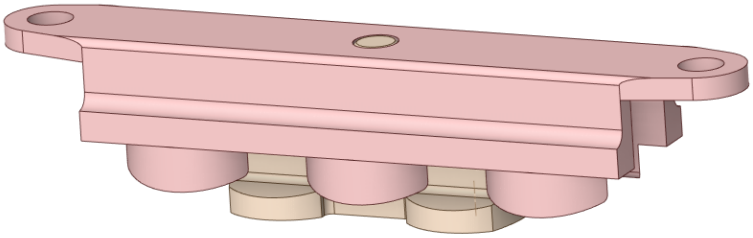

Fig. 3.8. Three plug node 3D model.

Roller section profile

The profile of the roller section is the main element of this equipment, serving as an element for fastening rollers, end locks, vertical fixators and three-plug units. It is made of aluminum alloy Д16Т with a wall thickness of 2 (mm). In highly loaded areas of the section profile, such as the area where the end lock is attached, and places susceptible to longitudinal bending wall thickness is locally increased, (fig. 3.11). In the places where the rollers are installed, and in the profile structure, there are stiffening ribs that help to avoid transverse bending of the wall of the roller section under the influence of loads. Also, in the places where the axes of the elements are installed, there are local thickenings in the walls designed to increase the contact area of the profile wall with the bushing, thereby increasing the ability of the wall to withstand bearing stresses. In places where vertical fixator and three-plug units are installed, there are also stiffening ribs, which are also the place where these units are fixed using threads, (fig 3.9. - fig 3.10.). Also, on the side of the roller opposite to the end lock there is a screw for fastening an additional module with two rollers.

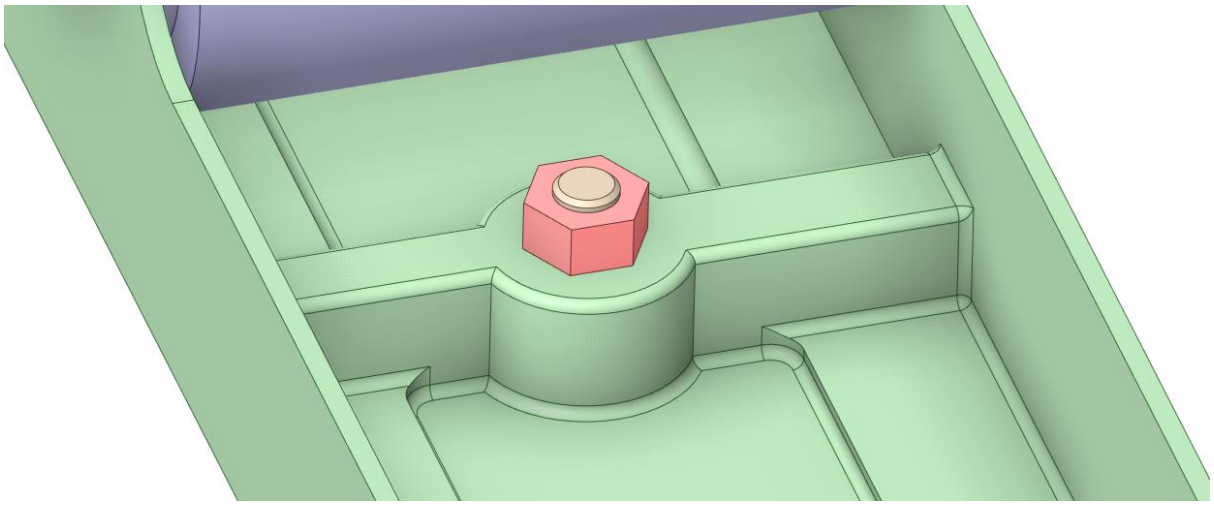

Fig. 3.9. Vertical fixation node installation 3D model.

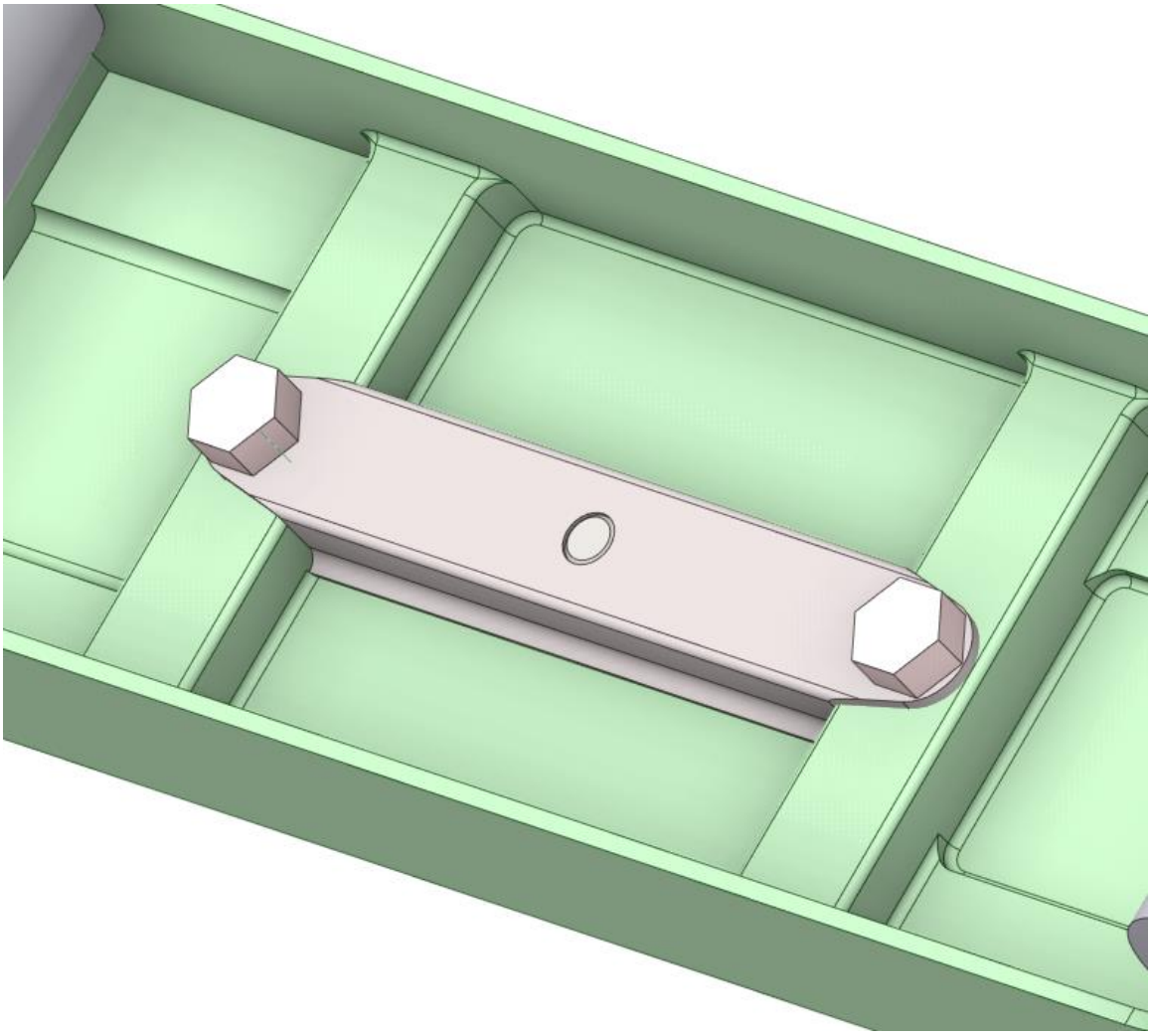

Fig. 3.10. Three plug node installation 3D model.

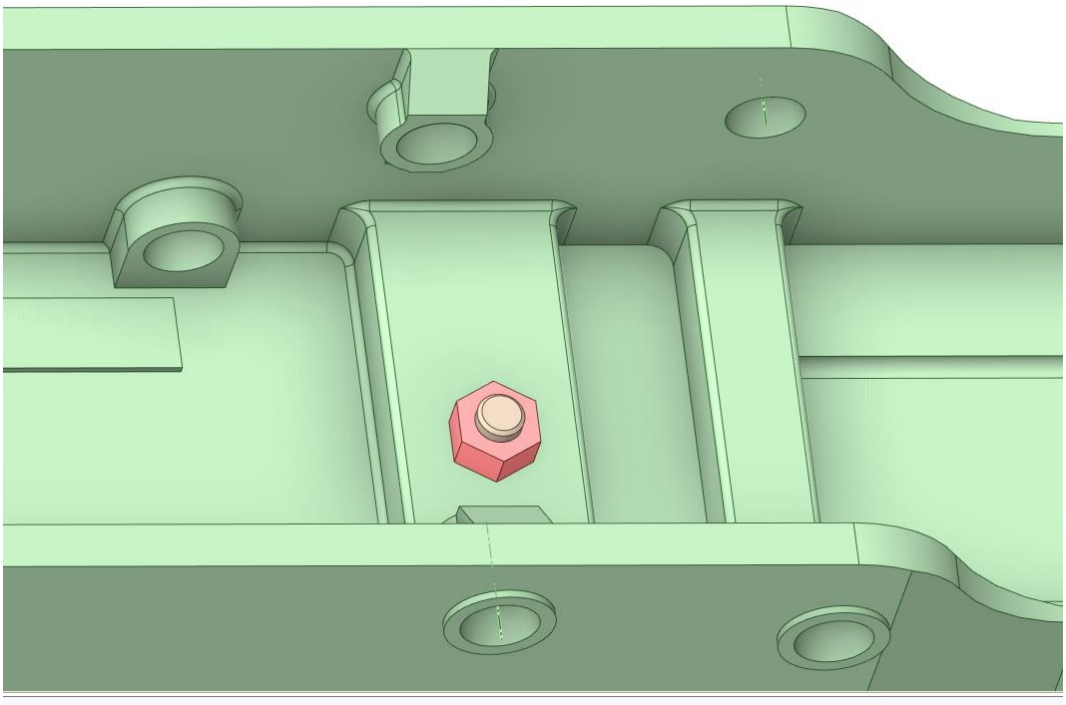

Fig. 3.11. End lock and vertical fixator installation points 3D model.

Additional module section

Additional module section is attachable to the main universal roller section by thread. It's main purpose is to increase the amount of rollers, and fill the gap between main sections to prevent the pallet's bottom sagging and potential damage due to it. It is equipped with two rollers, one vertical fixation node to fix the section in the seat rail. And a stiffness rib which is much thinner than the main section's one, because there are almost no vertical loads directed upwards in this section that can cause the profile to bend. The module section 3D model can be seen on figure 3.12.

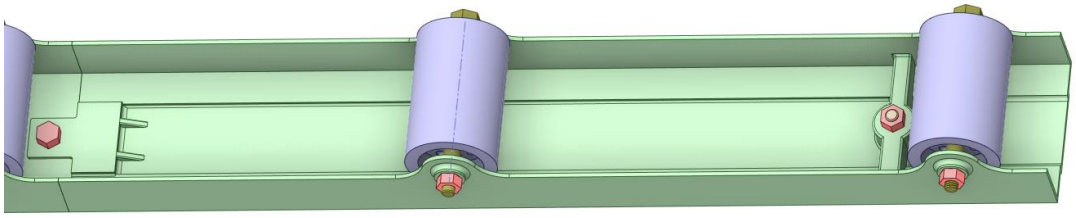

Fig. 3.12. Module section 3D model.

Assembly

The universal roller section assembly includes such components: 6 rollers, 6 roller bolts, 1 three-plug node, 2 vertical fixation nodes, 1 end lock. The assembly 3D model can be seen on figure 3.13.

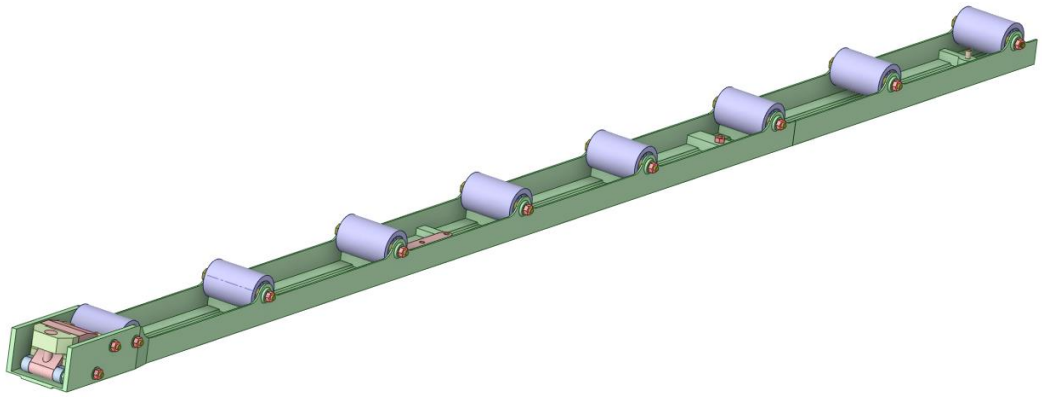

Fig. 3.13. Universal roller section with additional roller module 3D model.

3.3. Method of application, and cargo compartment loading variants with use of universal roller section.

Roller sections are installed in the cargo cabin in a configuration that depends on the type of cargo being transported. The roller sections are bidirectional, which means that for all loading variants, a section must be installed in a mirrored position relative to the center of the cargo to secure the load from the aft side. Since the allowable range of pallet center of gravity displacement can lead to uneven roller loading, for all loading configurations, the roller track section is installed so that the longitudinal edges of the cargo rest on the roller closest to the end lock, which has the largest reinforcement rib beneath it.

To transport pallets and containers with dimensions of 88×108 inches, eight roller sections are used per unit of cargo. To secure the load from the aft side, the roller section is installed with the lock side facing the tail. The longitudinal distance between the sections holding one unit of cargo in this case is 14 teeth of the seat rail. Variants for positioning the cargo when transporting 88×108 inch containers and pallets are shown on figure 3.14.

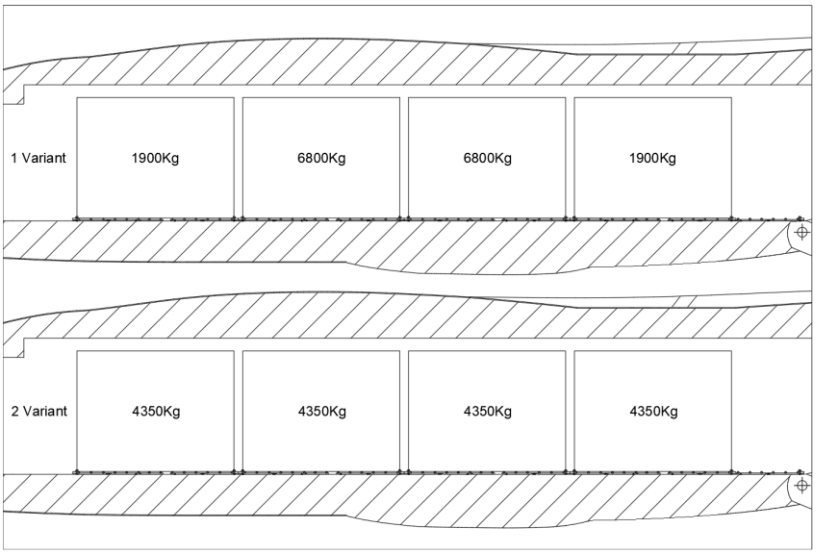

Fig 3.14. Variants for positioning the cargo with size of 88x108 inches.

To transport pallets and containers with dimensions of 96×108 inches, eight universal sections are used. Additionally, a modular section with two rollers is attached to the opposite side of the lock on one of the four sections to maintain the structural integrity of the pallet and prevent it from sagging between sections. In this configuration, the distance between sections, excluding the length of the additional section, will be 31 teeth of the seat rail. Variants for positioning the cargo when transporting 96×108 inch containers and pallets are shown on figure 3.15.

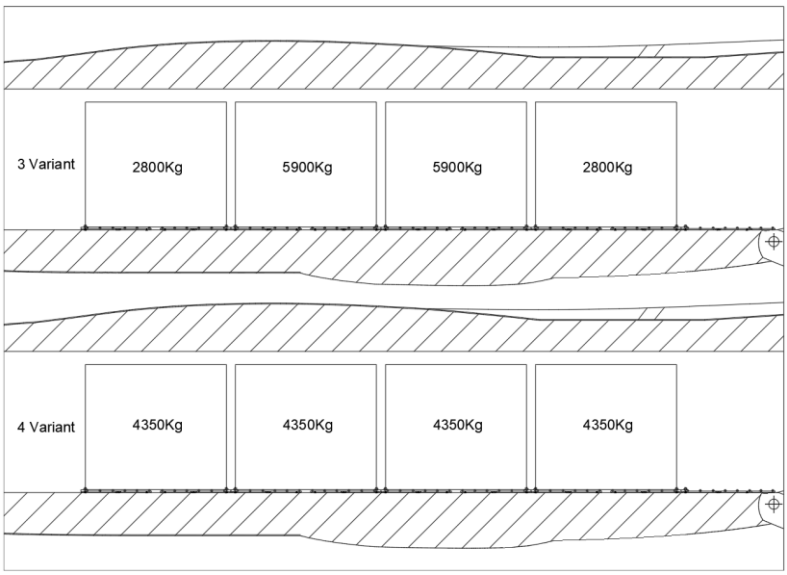

Fig. 3.15. Variants for positioning the cargo with size of 96×108 inches.

For transporting ISO containers as well as containers with dimensions of 96×238.5 inches, 16 universal roller sections with 8 additional sections are used. Additionally, 16 roller sections are necessary to ensure the transportation of cargo from the ramp to the fixation point to maintain proper centering. Furthermore, when transporting such types of cargo, the payload reserve allows for the placement of an additional 88×108 inch container. Although the transportation of such cargo types does not imply the use of end locks, the container should still be positioned so that its longitudinal edges rest on the first or second roller from the end lock. Options for positioning cargo when transporting 96×238.5 inch containers and pallets are shown on figure 3.16.

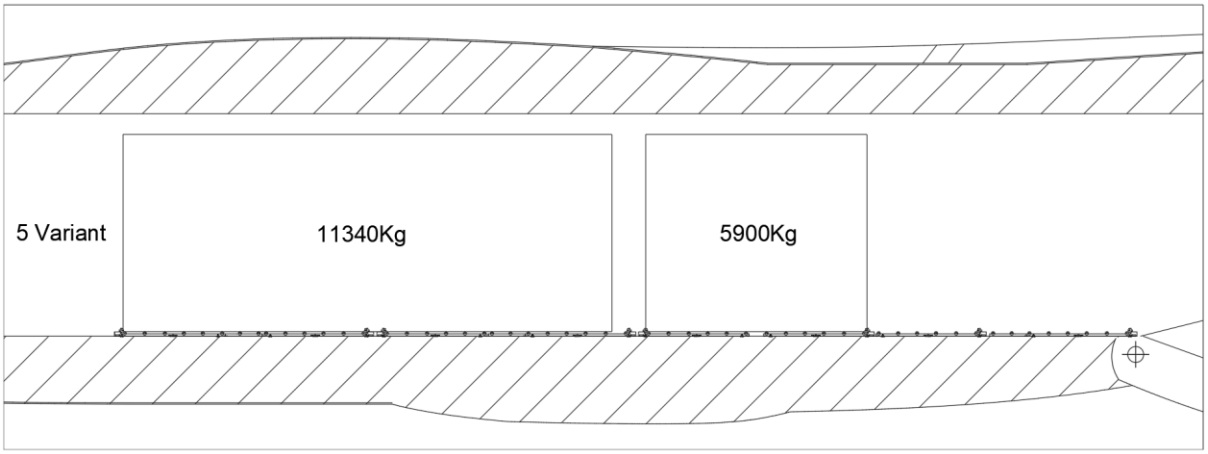

Fig. 3.16. Variants for positioning the cargo with sizes of 96×238.5 inches.

3.4. Static strength analysis of the universal roller section elements.

To analyze the static strength of the elements of the universal roller section, it is necessary to consider the maximum loads occurring during normal use of this equipment.

3.4.1. Roller assembly analysis

The maximum load on the roller is taken from the "Ansys" model (fig 3.17.) for 1 loading variant (fig. 3.14.). This load occurs during landing, under the influence of a vertical overload of 3.5 units, the center of gravity, which is shifted to the maximum values of the permissible range, namely 10% in the transverse direction,

5% in the longitudinal direction. If the mentioned factors coincide, the maximum load on the roller is: $P_Y^P = 9657$ (N) = 985 (kgf).

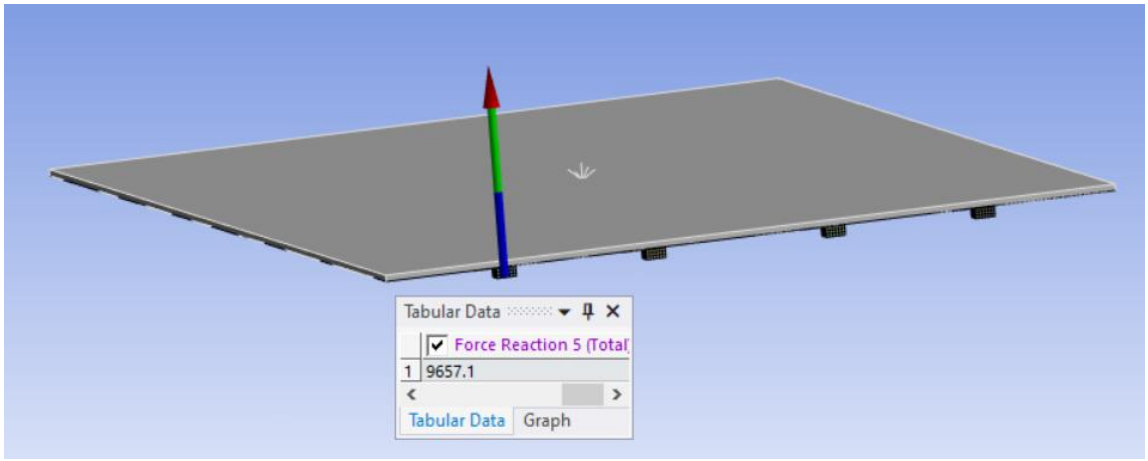

Fig. 3.17. Maximum load acting on a roller.

Bolt:

Material: 30ХГСА-Б

$\sigma_{ultimate} = 11000$ (kgf/cm^2);

$E_{steel} = 2100000$ (kgf/cm)^2;

Bushing:

Material: 12Х18Н10Т-Б

$\sigma_{ultimate} = 5500$ (kgf/cm^2);

$\sigma_{yield} = 2000$ (kgf/cm^2);

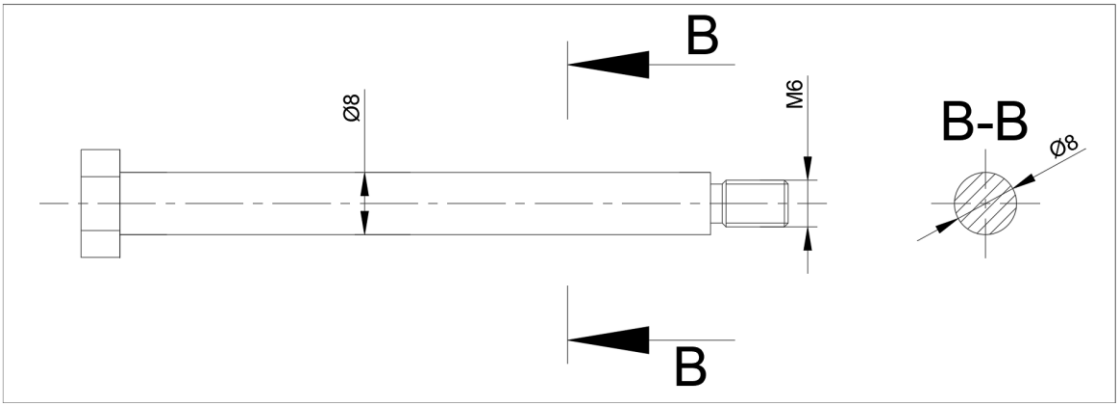

Fig. 3.18. Bolt cross-section.

To analyze the load-bearing capacity of a bolt, it is necessary to consider the loading scheme. Scheme is shown on figure 3.19.

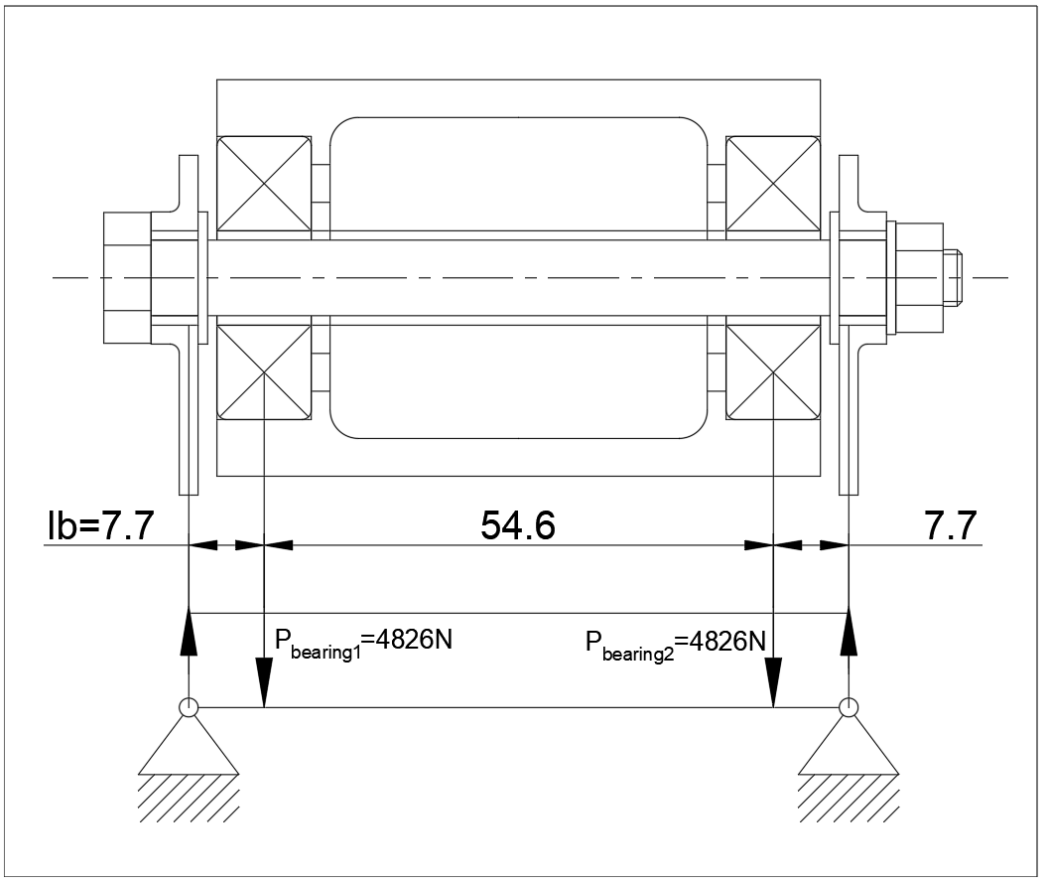

Fig. 3.19. Bolt loading scheme.

Since the bearings are equidistant from the center of the roller, the loads on them are divided equally:

$$P^{p}_{hinge1} = P^{p}_{hinge2} = \frac{P^{P}_{Y}}{2} = \frac{985}{2} = 492.5 \text{ (kgf)}.$$

Subsequently, the load from the bearing is transferred to the bolt, which leads to the occurrence of a bending moment, the maximum value of which is achieved in the area of the bolt coinciding with the center of the wall of the roller track profile.

The bending moment will be equal to the product of the force transmitted from the bearing to the bending arm:

$$M^{p}_{B-B\max} = P_{hinge1} \cdot l_B = 492.5 \cdot 0.77 = 379.23 \text{ (kgf} \cdot \text{cm)}.$$

Also, at the point where the bolt is attached to the profile, there is a bushing, which also takes part in the distribution of bending moment. To determine the portion of the load carried by the bushing, it is necessary to divide the bending moment in proportion to the moments of inertia of both elements. To do this, you need to determine the geometric characteristics of the sections of both elements.

Geometric characteristics of the bolt cross section:

Area of the B-B cross section:

$$F_{B-B} = F_{\varnothing 8} = \pi r^2 = 3.14 \cdot 0.4^2 = 0.5024 \ (\text{cm}^2).$$

Moment of inertia of cross section B-B:

$$I_{Б-Б} = I_{\varnothing 8} = \frac{\pi d^4}{64} = \frac{3.14 \cdot 0.8^4}{64} = 0.0201 \ (\text{cm}^4).$$

Cross section modulus B-B:

$$W_{B-B} = W_{\varnothing 8} = \frac{\pi d^3}{32} = \frac{3.14 \cdot 0.8^3}{32} = 0.0502 \ (\text{cm}^3).$$

Geometric characteristics of the bushing section:

Bushing cross-sectional area:

$$F_{bushing} = \pi\left(r_1^2 - r_2^2\right) = \pi\left(1^2 - 0.8^2\right) = 1 \ (\text{cm}^2).$$

Moment of inertia of the bushing in sections B-B:

$$I_{bushing} = \frac{\pi d_1^4}{64} - \frac{\pi d_2^4}{64} = \frac{3.14 \cdot 1^4}{64} - \frac{3.14 \cdot 0.8^4}{64} = 0.029 \ (\text{cm}^4).$$

Cross section modulus of the bushing in section B-B:

$$W_{bushing} = \frac{\pi \cdot \left(D^4 \cdot d^4\right)}{32 \cdot D^4} = \frac{\pi \cdot \left(1^4 \cdot 0.8^4\right)}{32 \cdot 1^4} = 0.058 \ (\text{cm}^3).$$

Also, to divide the bending moment, it is necessary to determine the Elastic Modulus of the bushing, taking into account that when the yield strength of the bushing is reached, the load is taken by the bolt:

$$E_{bushing} = \frac{\sigma_{yield} \cdot E_{steel}}{\sigma_{ultimate}} = \frac{2000 \cdot 2100000}{5500} = 763636 \ (\text{kgf/cm})^2.$$

Having calculated the geometric characteristics of the sections of the components, bending moment can be divide the in proportion to moments of inertia of elements using the formula:

$$M^{p}_{B-Bbushing} = \frac{M^{p}_{B-B\max} \cdot I_{bushing} \cdot E_{bushing}}{I_{bushing} \cdot E_{bushing} + I_{bolt} \cdot E_{bolt}},$$

$$M^{p}_{B-Bbushing} = \frac{379.23 \cdot 0,029 \cdot 764000}{0,029 \cdot 764000 + 0,0201 \cdot 2100000} = 130.42 \text{ (kgf} \cdot \text{cm)}.$$

In this case, portion of the bending moment taken by the bolt will be:

$$M^{p}_{B-Bbolt} = M^{p}_{B-B\max} - M^{p}_{B-Bbushing} = 379.23 - 130.42 = 249.81 \text{ (kgf} \cdot \text{cm)}.$$

We divide the shearing force in proportion to the ratio of the areas and the correction factor, which depends on the shape of the section.

Bolt section:

$$F_{B-Bbolt} \cdot \beta_1 = 0.5024 \cdot \frac{4}{3} = 0.67.$$

Bushing section:

$$F_{B-Bbushing} \cdot \beta_2 = 1 \cdot 2 = 2.$$

Coefficient of shear force distribution:

$$k = \frac{F_{B-Bbushing} \cdot \beta_2}{F_{B-Bbolt} \cdot \beta_1} = \frac{2}{0.67} = 3.$$

To determine the shear force arising in the components, we draw up an equilibrium equation:

$$P^{p}_{sh.bolt} + P^{p}_{sh.bushing} = P^{p}_{sh.bolt} + 3 \cdot P^{p}_{sh.bolt} = P^{p}_{hinge1} = 492 \text{ (kgf)}.$$

From this follows:

$$P^{p}_{sh.bolt} = 123.13 \text{ (kgf)},$$

$$P^{p}_{sh.bushing} = 369.38 \text{ (kgf)}.$$

Normal stresses in the section B-B of the bolt:

$$\sigma^{p}_{B-Bbolt} = \frac{M^{p}_{B-Bbolt}}{W_{B-B}} = \frac{249.81}{0.0502} = 4976.3 \text{ (kgf/cm}^2\text{)}.$$

Tangential stresses in the section B-B of the bolt:

$$\tau^{p}_{B-Bbolt} = \frac{P^{p}_{sh.bolt}}{F_{B-B}} = \frac{123.13}{0.5024} = 245.07 \text{ (kgf/cm}^2\text{)}.$$

To determine the equivalent stresses, we use the von Mises formula:

$$\sigma_{eq} = \sqrt{\sigma^{p}_{B-Bbolt}{}^{2} + 3 \cdot \tau^{p}_{B-Bbolt}{}^{2}} = \sqrt{4976.3^2 + 3 \cdot 245.07^2} = 4997 \text{ (kgf/cm}^2\text{)}.$$

Bolt safety factor:

$$\eta = \frac{\sigma_{ultimate}}{\sigma_{eq}} = \frac{11000}{4997} = 2.2.$$

Normal stresses in the section B-B of the bushing:

$$\sigma^{p}_{B-Bbushing} = \frac{M^{p}_{B-Bbushing}}{k \cdot W_{bushing}} = \frac{130.41}{1.4 \cdot 0.058} = 1603.45 \text{ (kgf/cm}^2\text{)}.$$

Ductility coefficient for bushing:

$$k = \frac{16}{3\pi} \cdot \frac{1-(d/D)^3}{1-(d/D)^4} = \frac{16}{3\pi} \cdot \frac{1-(0.8/1)^3}{1-(0.8/1)^4} = 1.4.$$

Tangential stresses in section B-B of the bushing:

$$\tau^{p}_{B-Bbushing} = \frac{P^{p}_{sh.bushing}}{F_{bushing}} = \frac{369.38}{1} = 369.38 \text{ (kgf/cm}^2\text{)}.$$

Equivalent stresses:

$$\sigma_{eq} = \sqrt{\sigma^{p}_{B-Bbushing}{}^{2} + 3 \cdot \tau^{p}_{B-Bbushing}{}^{2}} = \sqrt{1603.45^2 + 3 \cdot 369.38^2} = 1700.4 \text{ (kgf/cm}^2\text{)}.$$

Bushing safety factor:

$$\eta = \frac{\sigma_{ultimate}}{\sigma^{p}_{B-B}} = \frac{5500}{1700.4} = 3.23.$$

3.4.2. End lock analysis

Material 30ХГСА-Б

$\sigma_{ultimate} = 11000 \text{ (kgf/cm}^2\text{)}.$

The maximum end lock load values are taken from the "Ansys" Computer aided modeling environment.

Vertical loads on the end lock

Maximum longitudinal loading on end lock (fig. 3.20.) is experienced when transporting a load with a weight of 6800 kg with an overload of 2.4 units with a maximum permissible displacement of the center of gravity of the load in the transverse direction of 10%, in the longitudinal direction of 5%. It is also worth noting that crossbar locks installed in the lock beams also take part in the distribution of vertical loads, which reduces the load on the end lock by 4 times.

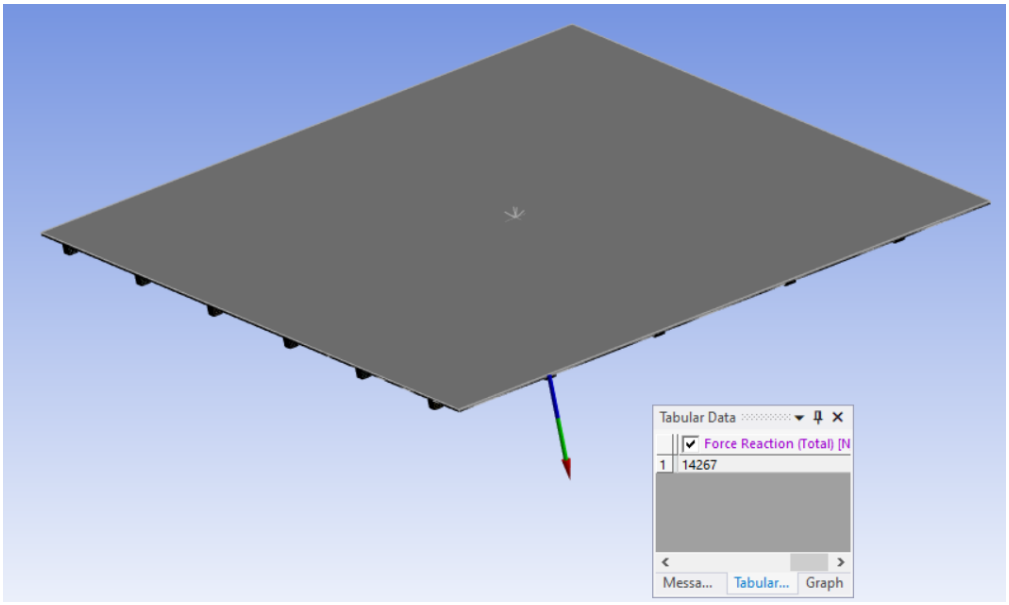

Fig. 3.20. Maximum load acting on a lock vertically.

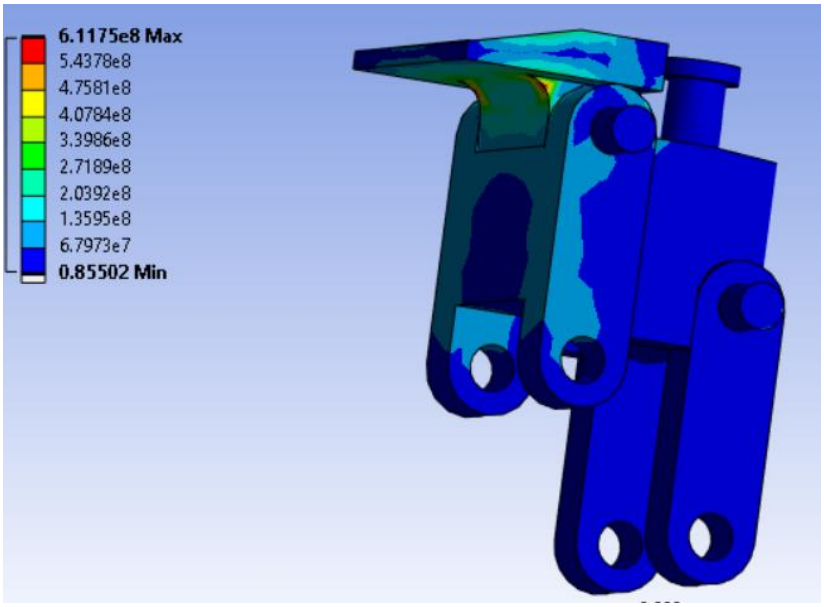

Fig. 3.21. Maximum stress in a lock during vertical loading.

$\sigma_{eq} = 611.7\ (\text{MPa}) = 5995\ (\text{kgf/sm}^2)$.

Safety factor

$$\eta = \frac{\sigma_{ultimate}}{\sigma_{eq}} = \frac{11000}{5995} = 1.83.$$

Longitudinal loads on the end lock

Maximum longitudinal load on end lock is experienced when transporting cargo weighing 6800 kg with an overload of 2.05 units with a maximum permissible displacement of the center of gravity of the cargo in the transverse direction of 10% (fig. 3.22.).

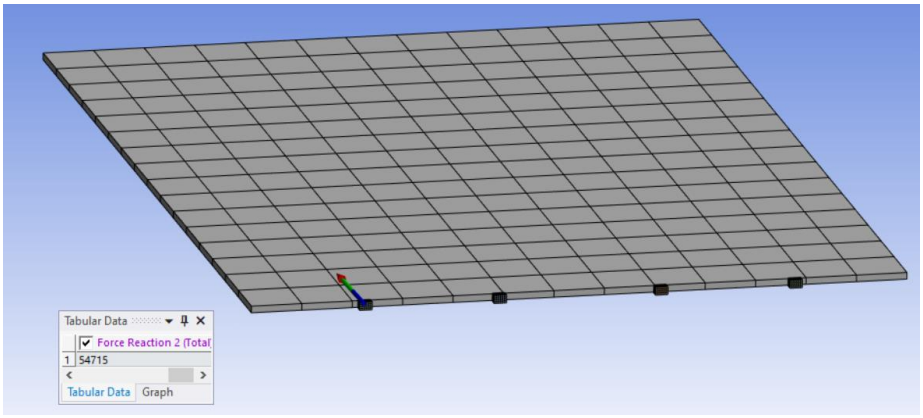

Fig. 3.22. Maximum load acting on a lock longitudinally.

Maximum longitudinal load on end lock $P^{p}_{Xlock} = 5583.1\ (\text{kgf})$.

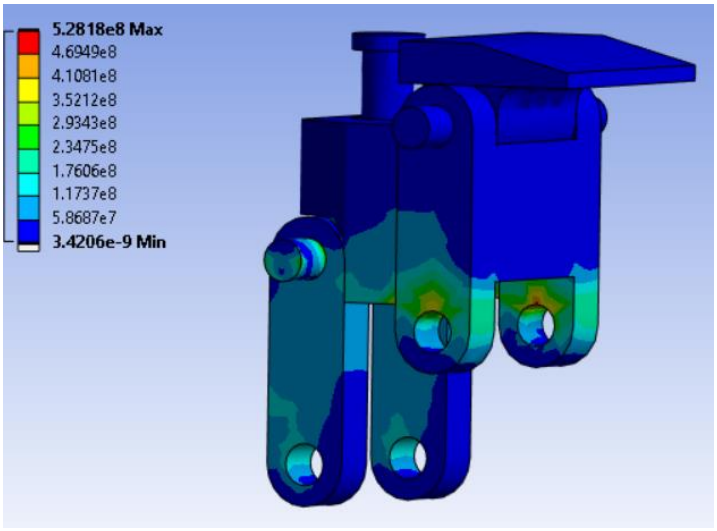

Fig. 3.23. Maximum stress during longitudinal loading.

$\sigma_{eq} = 528.2$ (MPa) $= 5176$ (kgf/cm^2).

Safety factor

$$\eta = \frac{\sigma_{ultimate}}{\sigma_{eq}} = \frac{11000}{5176} = 2.12 .$$

3.4.3. Analysis of the vertical fixation node

The maximum load acting on the vertical fixation node corresponds to the maximum value of the load acting on the end lock in the vertical direction:

$P^{p}_{Yfixator} = 14267$ (N) = 1455.8 (kgf).

In a vertical fixation node, there are two areas where the load causes the greatest stress. The first is the ear of the vertical fixation node, loading of which causes it to bend. The second is the thread of the vertical fixation node loading of which leads to tension.

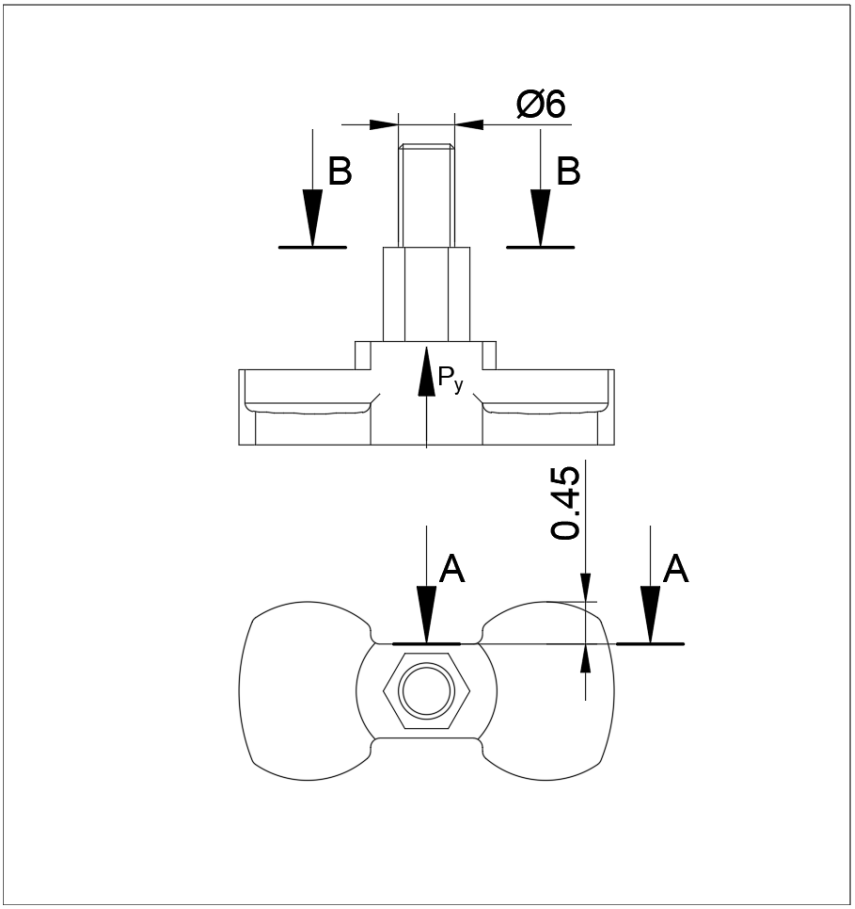

Fig. 3.24. Vertical fixator loading scheme.

A-A Cross section analysis

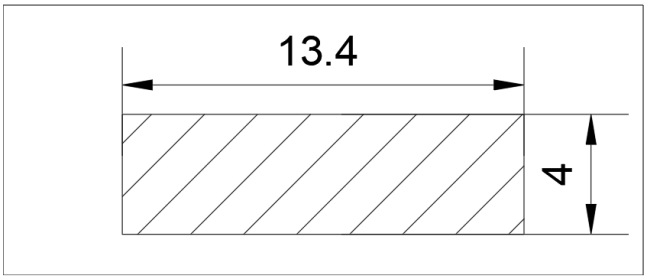

Fig. 3.25. Section A-A.

Bending moment is divided equally between the ears:

$$M^{p}_{A-A} = \frac{P^{p}_{Y}}{4} \cdot 0.45 = \frac{1455}{4} \cdot 0.45 = 163.7 \ (\text{kgf} \cdot \text{cm}).$$

Cross sectional area A-A:

$$F_{A-A} = 1.34 \cdot 0.4 = 0.54 \ (\text{cm}^2).$$

A-A cross section modulus:

$$W_{A-A} = \frac{0.4^2 \cdot 1.34}{6} = 0.036 \ (\text{cm}^3).$$

Normal stresses:

$$\sigma^{p}_{A-A} = \frac{M^{p}_{A-A}}{W_{A-A}} = \frac{163.7}{0.036} = 4580.8 \ (\text{kgf/cm}^2).$$

Tangential stresses:

$$\tau^{p}_{A-A} = \frac{P^{p}_{A}}{F_{A-A}} = \frac{163.7}{0.54} = 305.4 \ (\text{kgf/cm}^2).$$

Equivalent stresses:

$$\sigma_{eq} = \sqrt{{\sigma^{p}_{A-A}}^2 + 3 \cdot {\tau^{p}_{A-A}}^2} = \sqrt{4580.8^2 + 3 \cdot 305.4^2} = 4611.24 \ (\text{kgf/cm}^2).$$

Safety factor:

$$\eta = \frac{\sigma_{ultimate}}{\sigma_{eq}} = \frac{11000}{4611.24} = 2.39.$$

B-B Cross section analysis

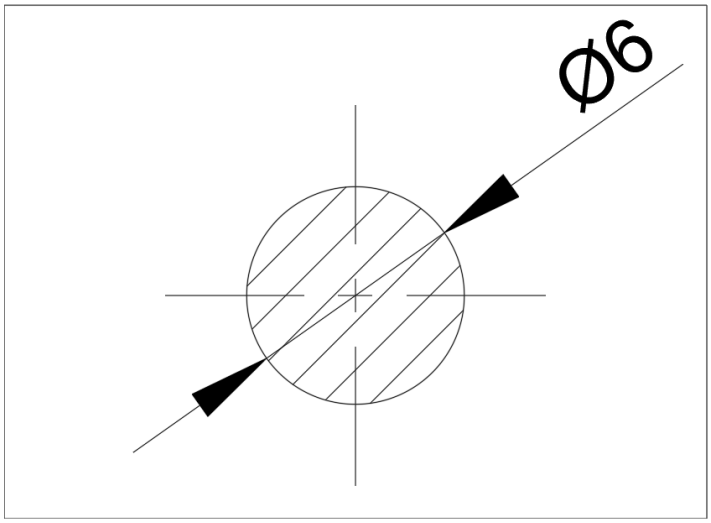

Fig. 3.26. Section B-B.

Sectional area B-B:

$$F_{B-B} = \pi \cdot 3^2 = 0.2827 \text{ (cm}^2\text{)}.$$

Shear stress:

$$\tau^p_{B-B} = \frac{P^p_A}{F_{B-B}} = \frac{1455}{0.2827} = 5148.6 \text{ (kgf/cm}^2\text{)}.$$

Safety factor taking into account threads in the section:

$$\eta = \frac{0.6 \cdot \sigma_{ultimate}}{\tau^p_{B-B}} = \frac{0.6 \cdot 11000}{5148.62} = 1.28.$$

3.4.4. Three-plug node analysis

Maximum force acting on a three plug node corresponds to the maximum longitudinal load on an end lock

$P^p_X = 5583 \text{ (kgf)} = 54715 \text{ (N)}.$

Maximum equivalent stress values occurring in three plug node a taken from the computer aided modeling environment "Ansys" (fig. 3.27.).

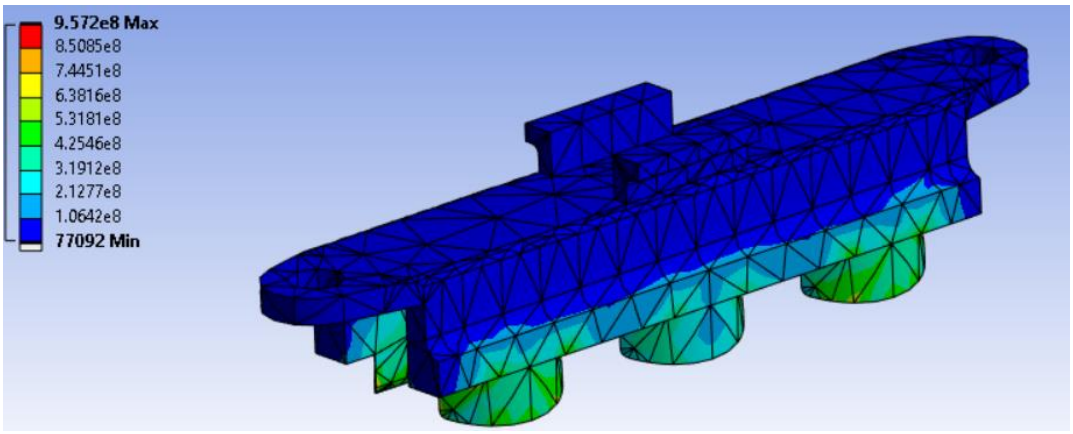

Fig. 3.27. Maximum equivalent stress in three plug node.

$\sigma_{eq} = 957.2\ (\text{MPa}) = 9750\ (\text{kgf/cm}^2)$.

Safety factor:

$$\eta = \frac{\sigma_{ultimate}}{\sigma_{eq}} = \frac{11000}{9750} = 1.12.$$

3.4.5. Roller section profile analysis

Material Д16Т.

$\sigma_{ultimate} = 4100\ (kgf\ /\ cm^2)$;

3.4.5.1. Bearing capacity of the roller track wall at the roller installation.

Load acting on the single wall of the roller track:

$$P^p_{Ywall} = \frac{P^p_Y}{2} = \frac{985}{2} = 492.5\ (\text{kgf}).$$

Bearing stresses resistance of the wall:

$$P_{bearing} = k \cdot \sigma_{ultimate} \cdot d \cdot \delta = 1 \cdot 4100 \cdot 1 \cdot 0.5 = 2050\ (\text{kgf}).$$

where: $k = 1$ – coefficient for fixed connections, d – bushing outer diameter,

δ – roller track wall thickness.

Safety factor:

$$\eta = \frac{P_{bearing}}{P^p_{Ywall}} = \frac{2050}{492.5} = 4.16.$$

3.4.5.2. Bending of the track profile under the roller.

Under each roller on the profile of the roller track there is a stiffness rib. The stiffness rib can be seen on figure 3.28.

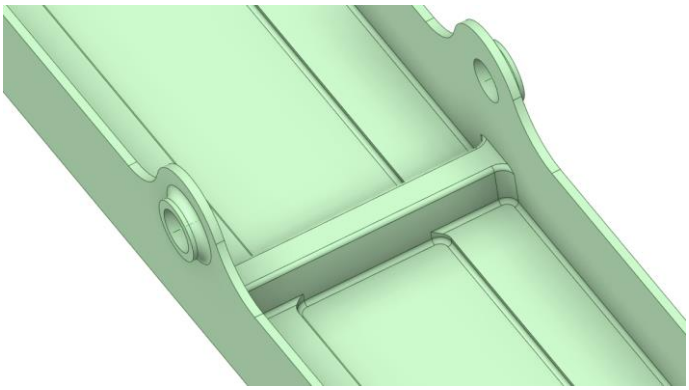

Fig. 3.28. Stiffness rib under the roller.

The width of the stiffness rib directly depends on the maximum load on the roller: $P^{p}_{Yroll} = 985$ (kgf).

To analyze the strength of roller profile it is necessary to consider the loading scheme (fig. 3.29.). The load acting on the roller is evenly distributed on both walls of the profile, which means the force acting on one wall is found according to the formula:

$$P^{p}_{Ywall} = \frac{P^{p}_{Yroll}}{2} = \frac{985}{2} = 490 \text{ (kgf)}.$$

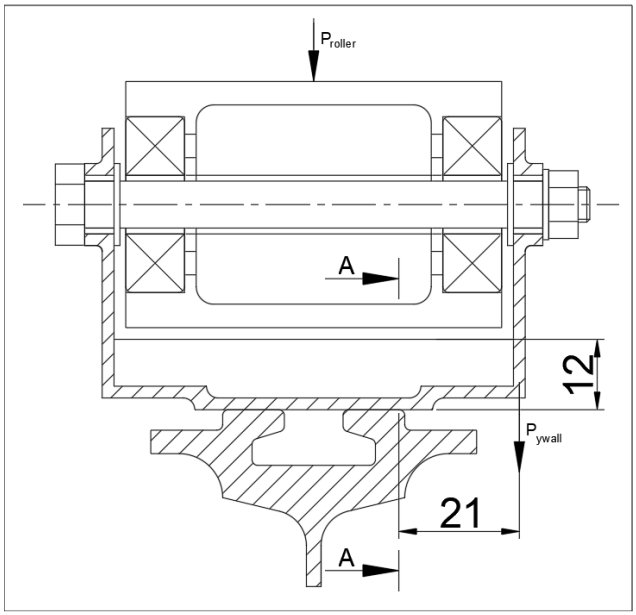

Fig. 3.29. Rib loading scheme.

Bending moment acting in section A-A:

$$M_{A-A}^{P} = P_{wall}^{p} \cdot l = 492.5 \cdot 2.1 = 1034.25 \text{ (kgf} \cdot \text{cm)}.$$

To determine stresses, it is necessary to estimate the geometric characteristics of section A-A. Section A-A can be seen on figure 3.30.

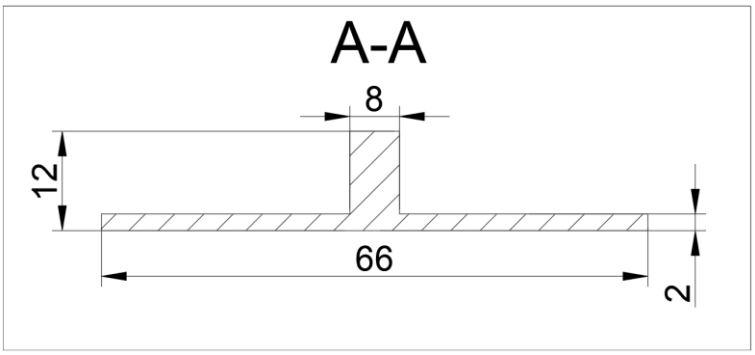

Fig. 3.30. Section A-A.

In order to determine geometrical properties of cross section it must be divided into 2 figures in order to determine their properties separately. Scheme of A-A section figures can be seen on figure 3.31.

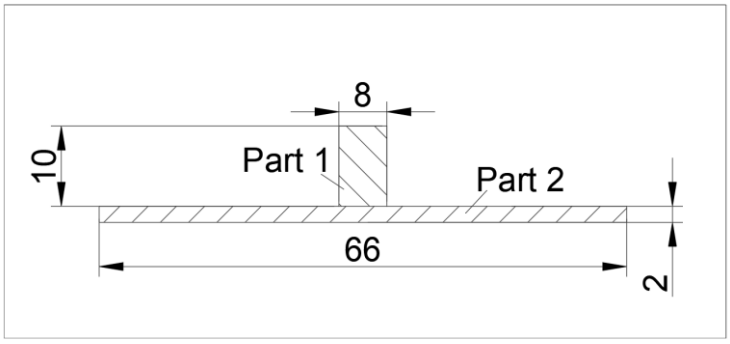

Fig. 3.31. Scheme of A-A section figures.

Areas of figures:

$$F_1 = 8 \cdot 10 = 80 \text{ (mm}^2\text{)},$$

$$F_2 = 66 \cdot 2 = 132 \text{ (mm}^2\text{)}.$$

The area of the entire section is the sum of its components:

$$F_1 = 8 \cdot 10 = 80 \text{ (mm}^2\text{)}.$$

Since the section is symmetrical horizontally, the determination of the centers of gravity of the figures must be carried out only vertically:

$$x_{c1} = \frac{10}{2} + 2 = 7 \text{ (mm)},$$

$$x_{c2} = \frac{2}{2} = 1 \text{ (mm)}.$$

Calculation of first moment of area for the cross-sections:

$$S_{x1} = 80 \cdot 7 = 560 \text{ (mm}^3\text{)},$$

$$S_{x2} = 132 \cdot 1 = 132 \text{ (mm}^3\text{)}.$$

Determining the center of gravity of a section:

$$x_c = \frac{560 + 132}{80 + 132} = 3.26 \text{ (mm)}.$$

Distances from the center of gravity of the figures to the center of gravity of the section:

$$\Delta x_{c1} = 7 - 3.26 = 3.74 \text{ (mm)},$$

$$\Delta x_{c2} = 3.26 - 1 = 2.26 \text{ (mm)}.$$

Figures moment of inerta:

$$I_{x1} = \frac{8 \cdot 12^3}{12} = 666 \text{ (mm}^4\text{)},$$

$$I_{x2} = \frac{66 \cdot 2^3}{12} = 44 \text{ (mm}^4\text{)}.$$

Section moment of inertia:

$$I_x = 666 + 80 \cdot 3.74^2 + 44 + 132 \cdot 2.26^2 = 2503.87 \text{ (mm}^4\text{)}.$$

Section modulus:

$$W = \frac{2503.87}{12 - 3.26} = 286.62 \text{ (mm}^3\text{)} = 0.29 \text{ (cm}^3\text{)}.$$

Normal stresses in a section created by a moment:

$$\sigma_{eq}^{p} = \frac{M_{A-A}^{p}}{W_{A-A}} = \frac{1034.25}{0.286} = 3608.4 \text{ (kgf/cm}^2\text{)}.$$

Safety factor:

$$\eta = \frac{\sigma_{ultimate}}{\sigma_{eq}^{p}} = \frac{4100}{3608.4} = 1.14 .$$

3.4.5.3. Bending of the roller track profile at the installation point of the vertical fixation node.

In order to perform the strength analysis it is necessary to consider the loading scheme, and cross section A-A. The section profile loading scheme at the installation point of vertical fixator can be seen on figure 3.32. The section A-A can be seen on figure 3.33

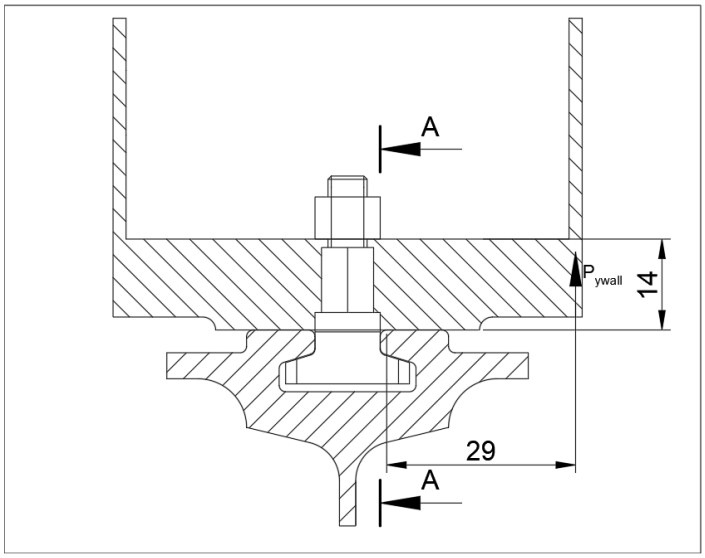

Fig. 3.32. Scheme of profile loading.

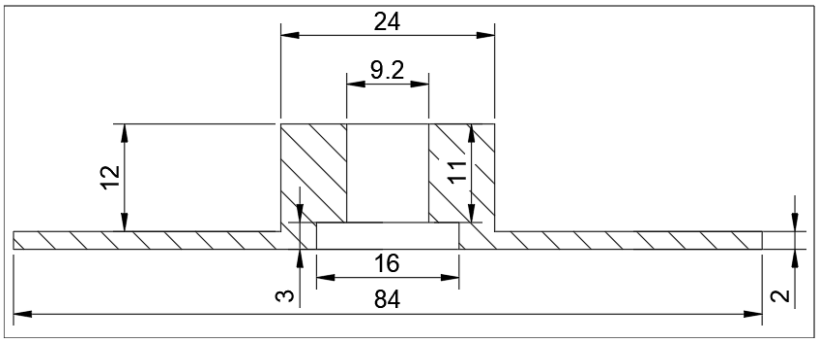

Fig. 3.33. Section A-A.

Geometric properties of section A-A:

In order to determine geometrical properties of cross section it must be divided into 4 figures which geometrical properties will be determined separately.

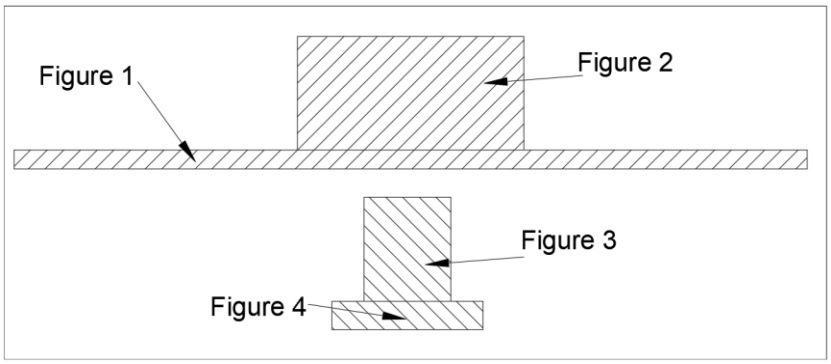

Fig. 3.34 Section A-A figures.

Note that figures 3 and 4 are cutouts, which means that in order to find geometrical properties of a section their individual properties should be subtracted from the properties of figures 1 and 2.

Areas of figures:

$$F_1 = 2 \cdot 84 = 168 \text{ (mm}^2\text{)},$$

$$F_2 = 12 \cdot 24 = 288 \text{ (mm}^2\text{)},$$

$$F_3 = 11 \cdot 9.2 = 101.2 \text{ (mm}^2\text{)},$$

$$F_4 = 3 \cdot 16 = 48 \text{ (mm}^2\text{)}.$$

Total cross-section area:

$$F_{A-A} = 168 + 268 - 101.2 - 48 = 306.8 \text{ (mm}^2\text{)}.$$

Coordinates of the center of mass of the figures:

$$x_{c1} = \frac{2}{2} = 1 \text{ (mm)},$$

$$x_{c2} = \frac{12}{2} + 2 = 8 \text{ (mm)},$$

$$x_{c3} = \frac{11}{2} + 3 = 8.5 \text{ (mm)},$$

$$x_{c4} = \frac{3}{2} = 1.5 \text{ (mm)}.$$

Calculation of first moment of area of figures:

$$S_{x1} = 1 \cdot 168 = 168 \text{ (mm}^3\text{)},$$

$$S_{x2} = 8 \cdot 288 = 2304 \text{ (mm}^3\text{)},$$

$$S_{x3} = 8.5 \cdot 101.2 = 860.2 \text{ (mm}^3\text{)},$$

$$S_{x4} = 48 \cdot 1.5 = 72 \text{ (mm}^3\text{)}.$$

Coordinate of the total section center of mass:

$$x_c = \frac{168 + 2304 - 860.2 - 72}{168 + 288 - 101.2 - 48} = 5.02 \text{ (mm)}.$$

Distance between the centers of mass of the section and figures:

$$\Delta x_{c1} = 5.02 - 1 = 4.02 \text{ (mm)},$$

$$\Delta x_{c2} = 8 - 5.02 = 2.98 \text{ (mm)},$$

$$\Delta x_{c3} = 8.5 - 5.02 = 3.48 \text{ (mm)},$$

$$\Delta x_{c4} = 5.02 - 1.5 = 3.52 \text{ (mm)}.$$

Moment of inertia of figures relatively to the center of mass:

$$I_{x1} = \frac{84 \cdot 2^3}{12} + 168 \cdot 4.02^2 = 2769.47 \text{ (mm}^4\text{)},$$

$$I_{x2} = \frac{24 \cdot 12^3}{12} + 288 \cdot 2.98^2 = 6015.44 \text{ (mm}^4\text{)},$$

$$I_{x3} = \frac{11 \cdot 9.2^3}{12} + 101.2 \cdot 3.48^2 = 2246.78 \text{ (mm}^4\text{)},$$

$$I_{x4} = \frac{16 \cdot 3^3}{12} + 48 \cdot 3.52^2 = 630.37 \text{ (mm}^4\text{)}.$$

Section moment of inertia:

$$I_{xA-A} = 2769.4 + 6015.44 - 2246.78 - 630.37 = 5907.76 \text{ (mm}^4\text{)}.$$

Section modulus is found by dividing the moment of inertia by the greatest distance from the center of section gravity to the edge:

$$W_{A-A} = \frac{5907.76}{2 + 12 - 5.02} = 657.8 \text{ (mm}^3\text{)} = 0.6578 \text{ (cm}^3\text{)}.$$

Maximum load on one profile wall:

$$P^{p}_{Ywall} = \frac{P^{p}_{Yfixator}}{2} = \frac{1455}{2} = 727.5 \text{ (kgf)}.$$

Bending moment:

$$M^{p}_{A-A} = P^{p}_{Ywall} \cdot l = 727.5 \cdot 2.9 = 2109.75 \text{ (kgf} \cdot \text{cm)}.$$

Normal stress:

$$\sigma^{p}_{A-A} = \frac{M^{p}_{A-A}}{W_{A-A}} = \frac{2109.75}{0.6578} = 3207.29 \text{ (kgf/cm}^2\text{)}.$$

Shear stress:

$$\tau^{p}_{A-A} = \frac{P^{p}_{A}}{F_{A-A}} = \frac{727.5}{3.068} = 237.13 \text{ (kgf/cm}^2\text{)}.$$

Equivalent stress:

$$\sigma_{eq} = \sqrt{{\sigma^{p}_{A-A}}^2 + 3 \cdot {\tau^{p}_{A-A}}^2} = \sqrt{3207.29^2 + 3 \cdot 237.13^2} = 3233.48 \text{ (kgf/cm}^2\text{)}.$$

Safety factor:

$$\eta = \frac{\sigma_{ultimate}}{\sigma_{eq}} = \frac{4100}{3233.48} = 1.27.$$

Conclusions to the special part

As a result of the work carried out, a section of roller floor equipment for the aircraft cargo cabin was created, which significantly simplifies the process of loading containers and pallets within the cabin and facilitates their securing during flight. The created section is universal and can be applied to all areas of the cargo cabin by attaching it to the seat rail.

During operation, non-standard situations can occur with the aircraft and its equipment, potentially leading to partial damage to its components. Creating standardized equipment elements significantly simplifies the process of addressing such damage by increasing the interchangeability of its components. Additionally, the universal section is sufficiently robust, as dictated by the need for the structure to withstand the full range of flight loads in various parts of the cargo cabin. While such equipment may be heavier than similar constructions, its strength reserve allows for flexibility in its application and adaptation for different types of cargo.

GENERAL CONCLUSIONS

1. The result of this project was the creation of a preliminary design for a short-haul cargo aircraft with a payload weight of 18 tons. The main geometric parameters of its structural elements were determined. Selected based on the expected technical characteristics of the aircraft in order to ensure maximum efficiency of the aircraft. All obtained values meet the requirements.

2. The Centering of the designed aircraft was carried out. In order to ensure maximum flight stability in accordance with the issued technical task. Drawings were created based on the aircraft chosen as the prototype, namely the An-178.

3. A unified section of aircraft cargo cabin equipment was developed to simplify the process of loading containers and pallets. Which also takes part in fixing it during the flight.

REFERENCES

1. Aviation Maintenance Technician Handbook FAA-H-8083-30A. Airframe. Volume 1. U.S. Department of Transportation. FAA, Flight Standards Service, 2018. https://www.faa.gov/sites/faa.gov/files/regulations_policies/handbooks_manuals/aviation/amt_general_handbook.pdf

2. Aviation Maintenance Technician Handbook FAA-H-8083-30A. Airframe. Volume 2. U.S. Department of Transportation. FAA, Flight Standards Service, 2018. https://www.faa.gov/sites/faa.gov/files/2022-06/amt_airframe_hb_vol_2.pdf

3. Kundu, A. K., Price, M., & Riordan, D. (2018). Conceptual Aircraft Design (1st ed.).Wiley.Retrieved fromhttps://www.perlego.com/book/992036/conceptual-aircraft-design-an-industrial approach-pdf (Original work published 2018)

4. Aircraft Design: A Conceptual Approach. 6th Edition by Daniel P. Raymer. Publisher: American institute of Aeronautics & Astraunatics. 2018.

5. Aircraft Design: A Systems Engineering Approach (Aerospace Series) 1st Edition, Kindle Edition by Mohammad H. Sadraey. Wiley, 2012.

6. General Aviation Aircraft Design: Applied Methods and Procedures Gudmundsson, S, Wiley, 2014.

7. Megson, T. H. G., Aircraft structures for engineering students, 7th edn, Butterworth-Heinemann,2021,ISBN978-0-12-822868-5. https://doi.org/10.1016/C2019-0-03113-5

8. Michael Chun Yung Niu. Airframe Stuctural Design. Practical Design Information and Data on Aircraft Structures 1988. https://www.academia.edu/15519222/Airframe_Structural_Design_by_Michael_Chung_Yung_Niu

					NAU 24 04L 00 00 00 05 EN		
	Sh.	№ doc.	Sign	Date			
Done by		Limanienko K.L.			References	list	sheet	sheets
Supervisor		Karuskevych M.V.				Q	62	68
St.control.		Krasnopolskyi V.S.				404 ASF 134		
Head of dep.		Yutskevych S.S.						

Appendix

Appendix A

Performed by: Limanienko Kyrylo
Supervisor: Karuskevych Mychailo

PRELIMINARY DESIGN OF THE AIRCRAFT
INITIAL DATA AND SELECTED PARAMETERS

Passenger Number	0.
Flight Crew Number	2.
Flight Attendant or Load Master Number	2.
Mass of Operational Items	1109.21 kg
Payload Mass	18000.00 kg
Cruising Speed	825. km/h
Cruising Mach Number	0.7754
Design Altitude	11.00 km
Flight Range with Maximum Payload	1500. km
Runway Length for the Base Aerodrome	2.55 km
Engine Number	2.
Thrust-to-weight Ratio in N/kg	2.7200
Pressure Ratio	22.00
Assumed Bypass Ratio	5.00
Optimal Bypass Ratio	5.00
Fuel-to-weight Ratio	0.2800
Aspect Ratio	11.00
Taper Ratio	3.50
Mean Thickness Ratio	0.120
Wing Sweepback at Quarter Chord	27.0 deg
High-lift Device Coefficient	0.970
Relative Area of Wing Extensions	0.010
Wing Airfoil Type – Supercritical	
Winglets – No	
Spoilers – Yes	
Fuselage Diameter	3.95 m
Fineness Ratio	8.16
Horizontal Tail Sweep Angle	35.0 deg
Vertical Tail Sweep Angle	40.0 deg

CALCULATION RESULTS

Optimal Lift Coefficient in the Design Cruising Flight Point	0.45377
Induce Drag Coefficient	0.00914

ESTIMATION OF THE COEFFICIENT Dm = Mcritical – Mcruise

Cruising Mach Number	0.77540
Wave Drag Mach Number	0.78050
Calculated Parameter Dm	0.00510

Wing Loading in kPa (for Full Wing Area):	
At Takeoff	4.340
At Middle of Cruising Flight	4.018
At the Beginning of Cruising Flight	4.178

Drag Coefficient of the Fuselage and Nacelles	0.00955
Drag Coefficient of the Wing and Tail Unit	0.00915
Drag Coefficient of the Airplane:	
At the Beginning of Cruising Flight	0.02921
At Middle of Cruising Flight	0.02885
Mean Lift Coefficient for the Ceiling Flight	0.45377
Mean Lift-to-drag Ratio	15.72932
Landing Lift Coefficient	1.584
Landing Lift Coefficient (at Stall Speed)	2.376
Takeoff Lift Coefficient (at Stall Speed)	1.980
Lift-off Lift Coefficient	1.445
Thrust-to-weight Ratio at the Beginning of Cruising Flight	0.619
Start Thrust-to-weight Ratio for Cruising Flight	2.745
Start Thrust-to-weight Ratio for Safe Takeoff	2.592
Design Thrust-to-weight Ratio	2.854
Ratio Dr = Rcruise / Rtake-off	1.059

SPECIFIC FUEL CONSUMPTIONS (in kg/kN*h):

Takeoff	38.7399
Cruising Flight	60.0369
Mean cruising for Given Range	60.5736

FUEL WEIGHT FRACTIONS:

Fuel Reserve	0.03466
Block Fuel	0.10766

WEIGHT FRACTIONS FOR PRINCIPAL ITEMS:

Wing	0.15145
Horizontal Tail	0.01752
Vertical Tail	0.02000
Landing Gear	0.02082
Power Plant	0.09300
Fuselage	0.13378
Equipment and Flight Control	0.12153
Additional Equipment	0.00346
Operational Items	0.01720
Fuel	0.14231
Payload	0.27908

Airplane Takeoff Weight	64997. kgf
Takeoff Thrust Required of the Engine	92.05 kN

Air Conditioning and Anti-icing Equipment Weight Fraction	0.0160
Passenger Equipment Weight Fraction (or Cargo Cabin Equipment)	0.0007
Interior Panels and Thermal/Acoustic Blanketing Weight Fraction	0.0072
Furnishing Equipment Weight Fraction	0.0233
Flight Control Weight Fraction	0.0066
Hydraulic System Weight Fraction	0.0177

Electrical Equipment Weight Fraction	0.0202	
Radar Weight Fraction	0.0058	
Navigation Equipment Weight Fraction	0.0087	
Radio Communication Equipment Weight Fraction	0.0044	
Instrument Equipment Weight Fraction	0.0102	
Fuel System Weight Fraction	0.0041	
Additional Equipment:		
Equipment for Container Loading	0.0000	
No typical Equipment Weight Fraction (Build-in Test Equipment for Fault Diagnosis, Additional Equipment of Passenger Cabin)	0.0035	
TAKE-OFF DISTANCE PARAMETERS		
Airplane Lift-off Speed	259.42	km/h
Acceleration during Takeoff Run	2.21	m/s*s
Airplane Take-off Run Distance	1082.	m
Airborne Take-off Distance	578.	m
Take-off Distance	1660.	m
CONTINUED TAKE-OFF DISTANCE PARAMETERS		
Decision Speed	236.95	km/h
Mean Acceleration for Continued Take-off on Wet Runway	0.27	m/s*s
Take-off Run Distance for Continued Take-off on Wet Runway	1814.84	m
Continued Take-off Distance	2393.22	m
Runway Length Required for Rejected Take-off	2480.37	m
LANDING DISTANCE PARAMETERS		
Airplane Maximum Landing Weight	60463.	kg
Time for Descent from Flight Level till Aerodrome Traffic Circuit Flight	21.9	min
Descent Distance	50.29	km
Approach Speed	248.04	km/h
Mean Vertical Speed	2.00	m/s
Airborne Landing Distance	516.	m
Landing Speed	233.04	km/h
Landing run distance	742.	m
Landing Distance	1258.	m
Runway Length Required for Regular Aerodrome	2101.	m
Runway Length Required for Alternate Aerodrome	1787.	m
ECONOMICAL EFFICIENCY		
The equipped aircraft mass to payload mass ratio	2.0614	
The mass of empty equipped aircraft per 1 passenger	0.00	kg/p
Relative performance with full load	347.65	km/h
Aircraft performance with maximum payload	12746.8	kg*km/h
Average time fuel consumption	3278.026	kg/h
Average distance fuel consumption	4.63	kg/km
Average fuel consumption for ton-kilometer	257.165	g/t*km
Average fuel consumption for passenger-kilometer	0.0000	g/p*km
Approximate evaluation of relative expenses for ton-km	0.2266	$/t*km

Appendix B

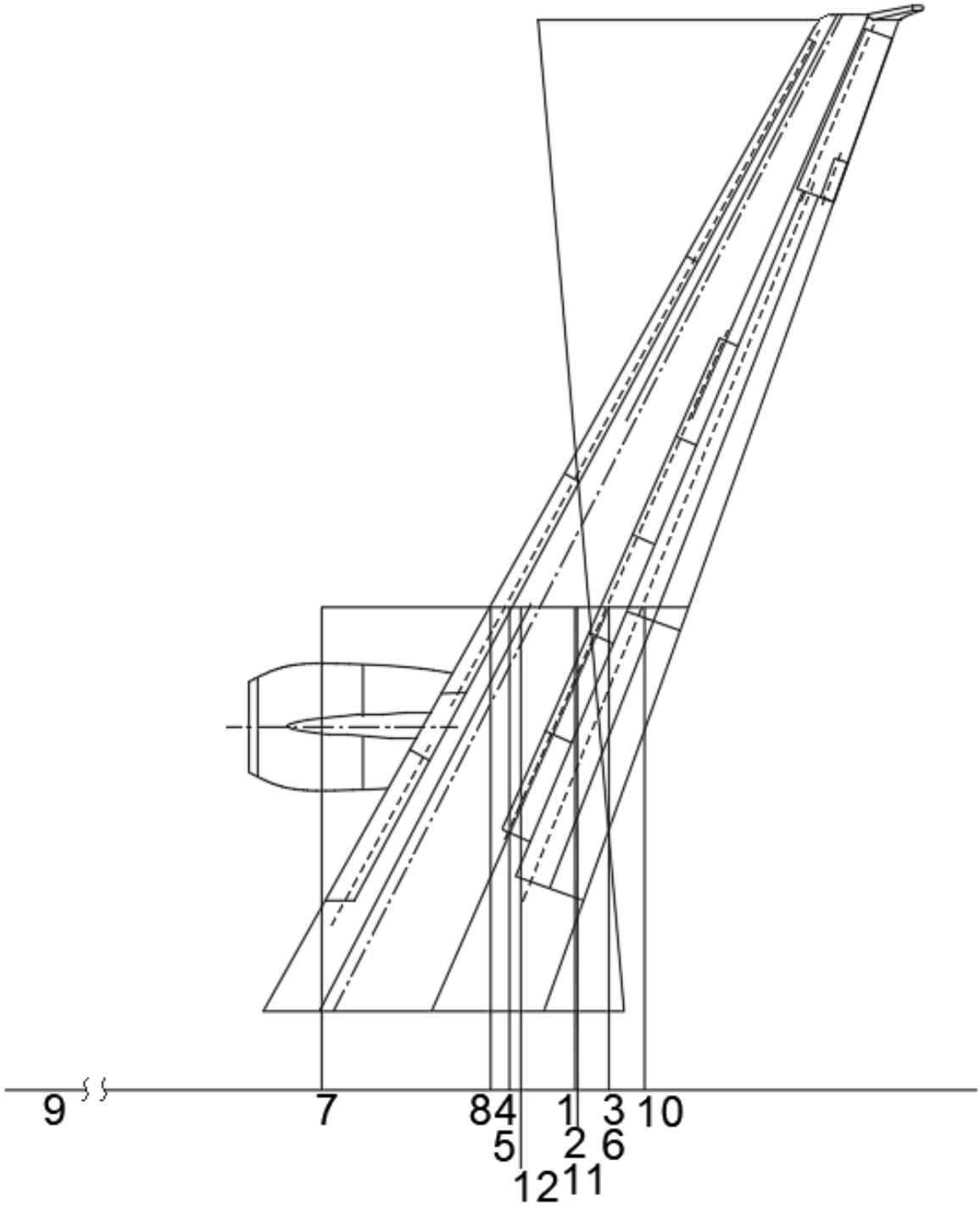

					NAU 24 04L 00 00 00 05	
Ch.	Sheet	Document №	Sign.	Date		Letter / Weight / Scale
Done by		Limanienko K. L.			Center of gravity of the wing	
Checked		Karyskevych M. V.				Sheet 1 / Sheet 2
St control		Krasnopolskyi V. S.			Appendix B	404 ASF 134
Head of dpt		Yutskevych S.S.				

Appendix C

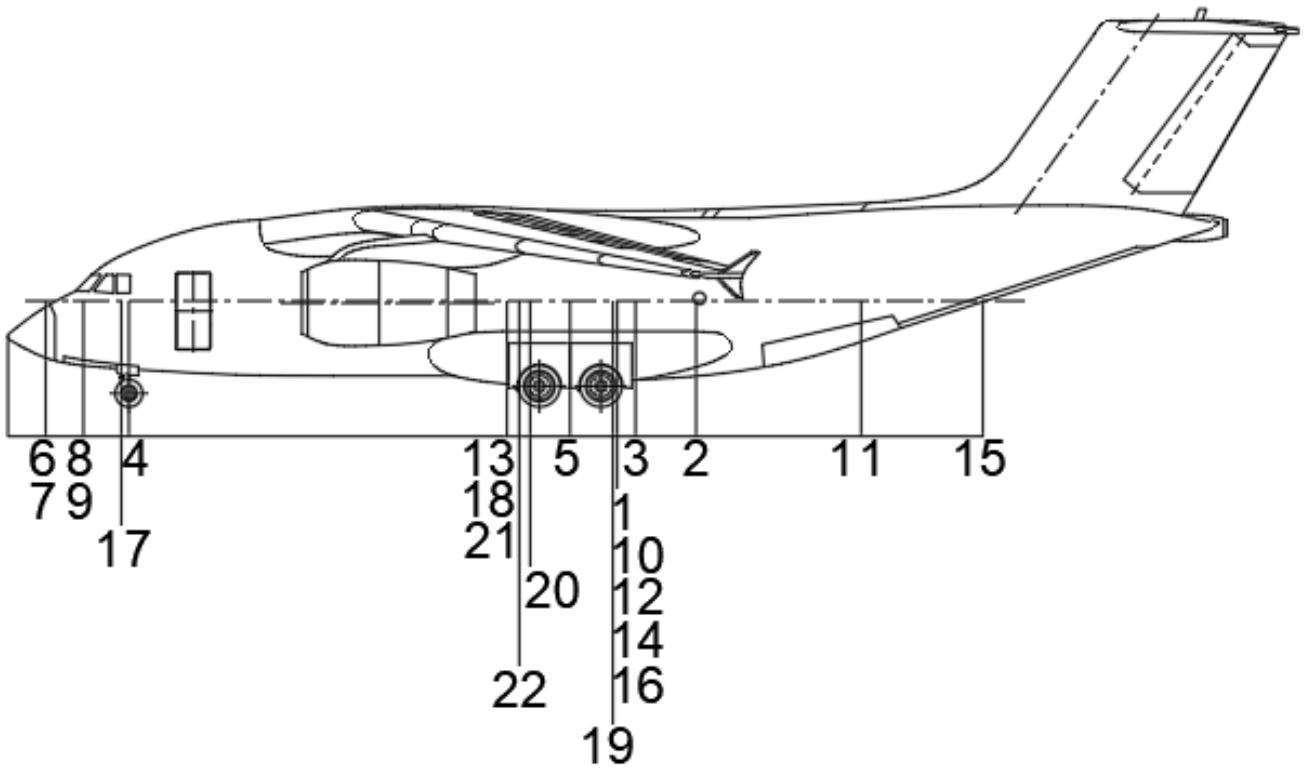

					NAU 24 04L 00 00 00 05	
Ch.	Sheet	Document	Sign.	Date		Letter / Weight / Scale
Done by		Limanienko K. L.			Center of gravity of the fuselage	
Checked		Karyakevych M. V.				Sheet 1 / Sheet 2
St control		Krasnopolskyi V. S.			Appendix C	404 ASF 134
Head of dpt		Yutskevych S.S.				